Solid Earth Discuss., https://doi.org/10.5194/se-2018-34
Manuscript under review for journal Solid Earth
Discussion started: 17 May 2018

Solid Earth Discussions
Open Access
EGU

Formation of linear planform chimneys controlled by preferential hydrocarbon leakage and anisotropic stresses in faulted fine-grained sediments, Offshore Angola

Sutieng Ho[1,5], Martin Hovland[2], Jean-Philippe Blouet[3], Andreas Wetzel[4], Patrice Imbert[5], and Daniel Carruthers[6]

[1]Department of Geosciences, National Taiwan University, P.O. Box 13-318, 106 Taipei, Taiwan
[2]Center for Geobiology, University of Bergen, Postboks 7803, N-5020 Bergen, Norway
[3]Fribourg University, Unite of Earth Sciences, Chemin du Musée 6, 1700 Fribourg, Switzerland
[4]University of Basel, Geological Institute, Bernoullistrassse 32, CH-4056 Basel, Switzerland
[5]Total-CSTJF, Avenue Larribau, Pau 64000, France
[6]Compagnie Générale de Géophysique, United Kingdom

Correspondence: Sutieng Ho (sutieng.ho@gmail.com), Jean-Philippe Blouet (jeanphilippe.blouet@gmail.com)

Abstract. A new type of gas chimney exhibiting unconventional linear planform has been observed on 3D seismic data offshore Angola, and is termed "Linear Chimneys". These chimneys occur in the shallow buried hemipelagic succession which was affected by syn-sedimentary remobilisation processes related to hydrocarbon migrations. Linear Chimneys are oriented parallel to the adjacent faults, within preferentially oriented tier-bound fault networks of diagenetic origin (also known as anisotropic Polygonal Faults, PFs) in the salt-deformational domain. These anisotropic PFs are parallel to salt-tectonic-related structures indicating their submission to horizontal stress perturbations generated by the latter. Only in anisotropic PF areas chimneys and their associated gas-related structures, e.g. methane-derived authigenic carbonates and pockmarks, show linear planforms. In areas without anisotropic PFs where the stress state is isotropic, gas expulsion structures of the same range of sizes exhibit circular geometry. In areas experiencing a transitional stress field, Linear Chimneys follow the trend of weak anisotropic PFs rather than the nearby tectonic structures. Therefore, the development of Linear Chimneys is interpreted to have been predominantly affected by the anisotropic stress field of PFs. The initiation of polygonal faulting formed 40 to 80 m below the seafloor and predates Linear Chimneys. The majority of Linear Chimneys nucleated at the lower part of the PF tier below the impermeable, upper portion of PFs, where gas accumulation was facilitated by a regional impermeable barrier. The permeable part of polygonal fault-bound traps is evidenced by PF cells filled with gas. These PF gas traps restricted the leakage points of overpressured gas-charged fluids to occur along the lower portion of PFs and hence, controlling the nucleation sites of chimneys. Gas leaking along the lower portion of PFs pre-configured the spatial organisation of chimneys. Anisotropic stress fields of tectonic and polygonal faults couple with partial impermeability of PFs determined directions of gas migration, linear geometry of chimneys, long term migration pathways and successive leaking events. Methane-related carbonates that precipitated above Linear Chimneys inherited the same linear planform geometry, both structures record the timing of gas leakage, the orientation of palaeo stress and thus can be used as a tool of stress reconstruction in sedimentary successions.

Solid Earth Discuss., https://doi.org/10.5194/se-2018-34
Manuscript under review for journal Solid Earth
Discussion started: 17 May 2018

1 Introduction

Hydrocarbon migration is directly impacted by structures such as faults and salt diapirs (Roberts and Carney, 1997; Talukder, 2012; Plaza-Faverola et al., 2012, 2015). Consequently, flow directions in the subsurface and utimately distribution of hydrocarbon leakage sites at the sea floor, are affected by such pre-existing structures (Thrasher et al., 1996; Moore et al., 1990). The morphology of structures formed during fluid leakage records style and intensity of fluid expulsion and thus, is useful for deciphering the fluid-migration history (Roberts et al., 2006; Blouet et al., 2017). 3D seismic reflection data has played an increasingly important role in visualisation, classification and evaluation of fluid flow features (Heggland, 1997). By conducting seismic analyses for vertical successions of fluid leakage expressions around faults, such as gas chimneys feeding pockmarks and seep carbonates, it is possible to unravel the timing and pathways of migrating fluids and the sealing efficiency of faults (Ligtenberg, 2005; Plaza-Faverola et al., 2012; Ho et al., 2016).

Recent studies from the upper slope of the Lower Congo Basin have revealed the existence of a new type of chimneys: In contrast to the usually observed circular chimneys, they are distinctly linear and display an extraordinary parallelism with tier-bound fault planes with polygonal organisation (Ho, 2013; Ho et al., 2016). Polygonal networks of discontinuities affecting discrete intervals of fine-grained sediment have been linked to diagenetic processes by Berkson et al. (1973), were first identified as tiered fault systems by Henriet et al. (1982; 1991; 1998) and investigated in detailed by Verschuren (1992). They were later called polygonal fault (PF) systems by (Cartwright, 1994) (see Clausen et al.; 1999; Goulty, 2008), although these faults can also be circular in map view (c.f. Chopra and Marfurt, 2007).

Hovland (1983) documented chimneys on high-resolution 2D-seismic data from the North Sea, exhibiting irregular elongate planform geometries with rounded summits, variable widths and lengths ranging between several hundred meters to more than one kilometre. They were interpreted as a result of escaping gas along fractures/faults from apices of underlying sedimentary folds (Hovland, 1983, 1984). Later, on 3D-seismic data, Hustoft et al. (2010) documented chimneys having elliptical cross-section and they were the first commenting on the planform ratio of chimneys. Hustoft et al. (2010) suggested that the preferred orientations of the long axis of horizontal sections of elliptical chimneys were caused by local stress perturbations associated with adjacent tectonic structures. In contrast to the chimneys described by (Hovland, 1983), the Linear Chimneys occurring in the Lower Congo Basin are string-like in plan-view. Furthermore, they vary little in width and have blunt terminations often with sharp tips. The Linear Chimneys are rooted along polygonal fault planes and align parallel with these. This geometrical arrangement suggests that the near-fault stress field affected the formation of the Linear Chimneys (Ho et al., 2012a). Previously, Ho (2013) and Ho et al. (2016) used intersecting positions of Linear Chimneys and PFs to determine the permeability of PFs, and suggested that overpressured gas-charged fluids cannot migrate further up of the fault plane to produce chimneys to escape. However, factors that determined the linear planform of these chimneys and their collective orientation have not been investigated, either why gas-charged fluid- migrated particularly into PF tier have not been explained.

Solid Earth Discuss., https://doi.org/10.5194/se-2018-34
Manuscript under review for journal Solid Earth
Discussion started: 17 May 2018

It has been known that stress-controlled orientations of venting structures and hydraulic fractures can redirect fluid flow (Nakamura, 1977; Plaza-Faverola et al., 2015). Detailed studies of the relationship between stress state, polygonal fault orientation, tectonic structures and injectites have been carried out by Bureau (2014); who demonstrated that sand injectites preferentially intrude pre-existing PFs along the extensional direction of adjacent tectonic structures. Nakamura (1977) studied interactions between orientation of magma fluid conduits and tectonic stresses. He established a conceptual framework relating the orientation of magmatic dykes to regional stress perturbations generated under different tectonic regimes; for instance, aligned zones of eruptions occur parallel to fault lines under extensional tectonic regimes, while zones of eruptions form at high angles with faults in compressive tectonic areas (Nakamura, 1977). Consequently, faulting and the near fault stress state can play an important role on fluid migration and, hence, on the formation and geometric development of fluid-flow generated structures.

Based on seismic observations, the objective of this study is to constrain the relative timing of fluid flow and polygonal faulting in shallow buried sediments thereby offering a fluid migration model for the affected interval in the study area. This model will be used as a platform to discuss the interactions between fluid flow, faults and local stress states. In particular the following questions are addressed why are chimneys linear in planform and not circular or elliptical as observed elsewhere, and why do they occur specifically along certain parts of PF planes?

2 Data and methods

Two 3D seismic surveys acquired in 2006 on behalf of Total over the outer shelf and upper slope of the Angolan continental margin (Lower Congo Basin) have been used. The larger of the two surveys covers an area of 1310 km² at about 1,000 m water depth (Fig. 1). The seismic data was obtained by using a dominant frequency of 55-60 Hz with a vertical resolution of approximately 7 m down to about 1s TWT below seafloor. The smaller survey within this area covers approximately 530 km² (Appendix 1). The dominant frequency was slightly higher (70-80 Hz) allowing to reach an improved vertical resolution of 5 m. Both 3D surveys have a bin size of 6.25 x 6.25 m and a map resolution of 6.25 m. The seismic data in both surveys has been post-stack time migrated and zero-phased. The data is displayed in SEG normal polarity where a downward increase in acoustic impedance is represented by wavelets of positive amplitude, shown on the figures in red. Near, middle, and far-offset volumes representing the amplitude of the signal received at different angles of incidence were used for verifying the presence of studied features, and to rule out whether they are seismic shadows of shallow anomalies or not. Here, data from the near offsets are shown as they yield the highest vertical resolution and are optimal for mapping the details of small fluid venting structures. Local horizons intersected by fluid venting structures were analyzed line-by-line and on arbitrary lines orthogonal to the structures to map e linear fluid venting structures most accurately. Furthermore, the studied chimneys were screened for potential artefacts, combining cross-section and map views, and were present in the aforementioned three types of seismic volumes.

Solid Earth Discuss., https://doi.org/10.5194/se-2018-34
Manuscript under review for journal Solid Earth
Discussion started: 17 May 2018

3 Geological setting

3.1 Regional setting

The Lower Congo Basin formed during rifting and breakup of western Gondwana followed by opening of the central South Atlantic (Mascle and Phillips, 1972). Two main phase of sedimentation can be distinguished: an Albian-Cenozoic passive margin sequence detached from a Neocomian-Aptian rift and sag sequences by Late Aptian evaporates (Fig. 2; Duval et al., 1992; Broucke et al., 2004). Since the end of salt deposition the passive margin sequence has been gravitationally unstable, incrementally translating seaward on Late Aptian evaporites (Duval et al., 1992). Translation was accommodated by upper slope extension and lower slope compression of the post-salt sediment cover. The 3D seismic survey is situated above the seaward end of this zone of extension comprising an assortment of minibasins and salt diapirs. This paper focusses on the relationship between fluid flow and geological structures in the upper passive margin sequence (Neogene-Quaternary). The principal units are summarized in Figure 2a.

3.2 Local tectono-stratigraphic framework

A large seaward-dipping listric growth fault rooted in the crest of a NW-SE trending salt wall divides the study area into a landward footwall domain and a seaward hanging wall domain (Ho, 2013). On the seaward side of the fault the Albian to early Cenozoic strata thicken into a turtle-back anticline (Fig. 2a). Four depocentres named Syncline 0, 1, 2, 3 occur on the NW, NE, SE and S sides of the anticline, respectively (Fig. 1). Synclines 0, 1 and 2 are located adjacent to two salt diapirs (D1 and D2; Fig. 1), which are rooted in the salt wall at depth. Syncline-0 subsided from the Early Miocene (c. 20 Ma) to Messinian (Ho, 2013). Synclines-1, and -2 subsided approximately since the early Middle Miocene (c. 16.4 Ma) until the Miocene-Pliocene (Ho, 2013). Some extensional faults in the SW side of Syncline-2, next to some chimney structures were still active during the Quaternary (Ho et al., 2012a, fig. 6b). The roll-over Syncline-3 in the south of the study area was induced by salt deflation during the Early Pliocene and became inactive in the Late Pliocene (Ho, 2013). The intervals containing fluid flow structures are located within the Middle Miocene to Quaternary strata being composed mainly of hemipelagic mudstone (Philippe, 2000), and intercalated with mass transport complexes (Fig. 2b). Particularly, the studied chimneys primarily occur within the Upper Miocene and Pliocene deposits and in syncline areas (Fig. 2b). These intervals are both deformed by arrays of polygonal faults named here as Tier-1 and Tier-2 (Ho et al., 2012a, 2013, 2016; Ho, 2013). PFs often extend into strata above (e.g. interval A in Fig. 3a). Strata immediately overlying the PF intervals cover the relied of the underling horst and graben structures with an isopach thickness (e.g. interval B-C in Fig. 3a). In Tier-2, a regional impermeable barrier called Intra-Pliocene has been identified by its geophysical character and immediately below which a vast distribution of gas accumulations is observed (Ho, 2013). The stratigraphic position of venting structures is summarized in Figure 2b.

Solid Earth Discuss., https://doi.org/10.5194/se-2018-34
Manuscript under review for journal Solid Earth
Discussion started: 17 May 2018

4 Observations

Evidence for fluid flow around salt structures is provided by the occurrences of chimneys, pockmarks, depressions, positive high amplitude anomalies (PHAAs) interpreted as methane-derived authigenic carbonates, and negative high amplitude (NHA) anomalies interpreted as free gas (Coffeen, 1978; Petersen, 2010; Plaza-Faverola et al., 2011; Ho et al., 2012a). These structures are characterised by a linear-to-circular geometry in plan view (Fig. 2b).

4.1 Linear Chimneys

4.1.1 Acoustic properties of Linear Chimneys and terminations

On seismic records, chimneys have been identified in worldwide locations (cf. Loseth et al., 2011; Berndt et al., 2003; Hustoft et al., 2010; Plaza-Faverola et al., 2010; Ho et al., 2016). Seismic chimneys are represented by narrow vertical zones characterised by either stacked amplitude anomalies, pull-up, push-down or distorted reflections (Heggland, 2005; Hustoft et al., 2007, 2010; Petersen, 2010; Loseth et al., 2001, 2011). In the study area Linear Chimneys are often associated with high-amplitude patches and flat-bottomed shallow depressions, all of these pile up to form vertical successions (Ho et al., 2012a). Linear Chimneys are typically expressed as "squeezed elongate columns" of acoustic distortion zones in seismic data, in plan-view as linear low-amplitude zones being 10s to 100s m wide and having an aspect ratio of 1:4 (Fig. 4a-b Ho et al., 2012a). Chimneys may terminate up- or downward into NHA patches (see map view and section in Fig. 4c-e), upward into linear flame-like patterns of PHAA (see map view and section in Fig. 5a), or linear, elongate or sub-circular shallow depressions on the modern seafloor (Fig. 5b). These three elements can be combined to form 3 key variations of vertical stacking sequences (Fig. 2b):

Type-1 Linear Chimneys terminate upwards into linear, PHAAs within depressions, which are shallow flat-bottomed with relief in the range 3-5 ms TWT (Fig. 5a-iii). The acoustic columns defining the chimneys are often associated with velocity pull-up effects (Appendix 2).

Type-2 Linear Chimneys terminate upwards into columns of NHA (Fig. 4c, d; Appendix 2). The chimney body is characterised by push-down reflection zones.

Type-3 Linear Chimneys terminate upwards into PHAAs with depressions and downwards into a NHA column (Fig. 6; Appendix 2). Linear Chimneys of this type are usually not represented by any reflection distortion zone. The NHA columns are situated in the lower part of the fault tier and are capped by the Intra-Pliocene regional barrier.

The topmost termination of a chimney is easy to distinguish when it is associated with pockmarks or PHAAs (cf. Heggland, 1997; Judd and Hovland, 2007; Cathles et al., 2010); while identifying the lower termination is challenging due to signal perturbations that increase with depth (Hustoft et al., 2007, 2009). Apart from the downward terminations of Type-3 chimney that can be clearly distinguished due to the NHA column, the two other types are poorly constrained. (Hustoft et al., 2007, 2010) suggested that the base of the chimney is marked by the disappearance of distorted seismic reflections. In this study, the lower tip of chimneys is considered to be located at the level where columns of distorted seismic reflections start to branch out in opposite directions (Fig. 4d) or where distortions disappear (Fig. 4c).

Solid Earth Discuss., https://doi.org/10.5194/se-2018-34
Manuscript under review for journal Solid Earth
Discussion started: 17 May 2018

4.1.2 Linear Chimneys and fault patterns

In the study area, Linear Chimneys occur within the Pliocene PF tier (Tier-2, Ho, 2013). They are parallel to PFs that have preferential directions. Both elements are often parallel to adjacent tectonic faults or salt structures (Figs. 1, 4a-b). PFs that follow the trends of tectonic structures and are several times longer than these smaller ones between them, are anisotropic; they are termed first-order PFs while the latter are second-order PF (Fig. 4a; Carruthers, 2012; Ho, 2013). There are three main groups of anisotropic PF arrays (see Appendix 3; Ho et al., 2013):

1) Concentric faults surrounding pockmarks (Ho, 2013, fig. 2a) or paralleling extensional faults of synclines (red dotted lines in Fig. 4c).

2) Radial faults occurring around salt diapirs (Appendix 3c) (Carruthers, 2012).

3) A ladder-like fault pattern occurring above Syncline-2 (Fig. 6a-b, Appendix 3d), found inside the area bounded by a set of concentric faults.

Although Linear Chimneys are often parallel to the first-order PFs (Fig. 4a, b) some linear conduits do not show preferred orientations at the NNE edge of Sycline-2 (Fig. 6a) where concentric and uni-directional PF arrays intersect. At this location PFs are more isotropically arranged (Fig. 6b). Another exception occurs above Syncline-1, where linear venting structures are parallel to the second-order PFs (see Appendix 4).

Few types of gas-charged fluid migration features are found within anisotropic PF networks. In the interval of PF Tier-2, in map view, a kilometric-scale PF area is filled by negative high amplitude patches in Syncline-3 (Fig. 4e), where NHA anomaly lumps are observed to reminiscent the PF pattern. The whole NHA area is limited laterally by the extensional fault of Sycline-3 and vertically by the Intra-Pliocene horizon, below which Linear Chimneys of Type-2 are observed (Fig. 4d).

Linear Chimneys are observed to intersect fault planes in different positions within PF Tier-2. A catalogue and a statistical analysis comprising counts of how common each intersection position, has been made by examining 209 detected chimneys (Fig. 7a; see also Appendix 2; sourced from Ho (2013), 2013; (Ho et al., 2016)). The Linear Chimneys intersecting PFs can be split into three main populations based on the number of their positions (Fig. 7b): (1) 54% intersect the lower part or basal tips of a single or a conjugate PFs, rise from the lower footwall/horst of PF, (2) 19% stem from (around) the intersection of pairs of conjugate PFs and occur along the middle of the PF hanging wall/grabens, and (3) 9% intersect the middle to upper portion of PFs, across both footwall and hanging wall.

Population (1) and (2) represents 73% of the total number of chimneys, and are the majority. In the case of population (2), the Linear Chimneys may also intersect the lower part of the PFs, but the seismic resolution and distortion prevents an accurate determination of their position. The remaining 17% intersect at various positions (Fig. 7b; Appendix 2). Furthermore, among the 73% (Fig. 7b), 23% and 8% of the chimneys terminate downwards into negative bright spots in the PF's footwall or hanging wall, respectively; all of them belong to Type-3 linear vents. Consequently, one-third of the chimneys are associated with free gas stored in the lower part of PF blocks, while the rest only have apparent roots in the lower part of the PF tier or deeper.

Solid Earth Discuss., https://doi.org/10.5194/se-2018-34
Manuscript under review for journal Solid Earth
Discussion started: 17 May 2018

4.1.3 Radial high-amplitude depression networks along salt-related faults

Although most linear venting structures occur in PF Tier-2, some exceptions occur. For example, a radial network was found along syncline-related extensional faults in a deeper Late-Middle Miocene interval devoid of PFs (for details see Fig. 8). This complex network is composed of interconnected linear depressions associated with PHAAs that overlie a Linear Chimney network (Fig. 8a-b). The Linear Chimneys are characterised by push-downs (Fig. 8c). The longest linear features occur along the strike of extensional faults.

5 Interpretation and discussion

The geometrical coincidence of Linear Chimney and PFs implies a relationship between both structures. To decipher the genetic relationships the following aspects need to be discussed: 1) the timing of PFs and Linear Chimney formation in respect to each other, 2) the gas-charged fluid migration pathway to the nucleated location of chimneys, 3) the mechanisms of preferential gas accumulation location, 4) factors that control the linear planform of the chimneys. Then a conceptual model for Linear Chimney formation will be proposed, followed by a demonstration of using Linear Chimneys for application in hydrocarbon exploration.

5.1 Timing of polygonal faulting

Analysing timing of polygonal fault's formation is essential for the discussion of whether pre-existing PFs affected fluid migration pathways, i.e. chimneys. The relationship between the timing of PFs and Linear Chimney formation can be constrained by several lines of evidence. Polygonal fault nucleation is widely considered to occur during the early stages of fine-grained sediment compaction (see Goulty, 2008). Authors like Berndt et al. (2012), Ostanin et al. (2012) and Carruthers (2012) suggested that PFs formed in shallow sub-seafloor sediments and ceased propagating when they tip out on the seafloor. Polygonal faults in the Neogene-Quaternary deposits of Lake Superior, Hatton Basin and Vøring Basin, demonstrate that their growth is very recent and could even occur to the present day seafloor (Berkson et al., 1973; Jacobs, 2006; Berndt et al., 2012; Laurent et al., 2012). Recently (Sonnenberg et al. , 2016) confirmed that PFs grew close to the seafloor with evidence of fault scarps filled by onlapping strata, syn-sedimentary. The non-uniform topmost terminations of PFs indicate upward propagation after PF initiation (Berndt et al., 2012).

Within the study area, new evidence was found to support that PFs grew in sediment very close to the palaeo seafloor. A previous study documents the syn-sedimentary growth wedge of Tier-2, buried ca. 50 ms below the modern sea floor (see Appendix 5; Ho, 2013), in which PFs disappeared progressively toward the pinch-out where the thickness decrease below 60ms. This means that PFs started to grow below seafloor at shallow depth: minimum 60 ms TWT (faulting during the tier deposition), or, maximum 110 ms TWT (faulting at present day). Similarly, timing evidence of PF faulting is shown in Tier-1. Onlapping reflections in the sedimentary layer covering a dome underlain by a circular PF-bounded horst (interval C in Fig.3C) indicates the synsedimentary formation (or reactivation) of the PFs. Knowing that the onlapping strata are located 80 ms above Tier-1,

Solid Earth Discuss., https://doi.org/10.5194/se-2018-34
Manuscript under review for journal Solid Earth
Discussion started: 17 May 2018

this dates the latest activity of the PFs subsequent to Tier-1 deposition. It can be observed that the particular PFs bounding the circular horst are significantly longer than most other PFs, and propagate largely above Tier-1 (into interval A in Fig. 3C). Thus, it is likely that most PFs formed during Tier-1 deposition, and some were reactivated once after the tier was buried (below interval A) at shallow depth (15ms below the seafloor). To conclude, based on literature and our seismic observations, the top-most boundary of both PF tiers represent approximately the timeline when the main tier cessed to form.

5.2 Formation of Linear Chimneys

Seismically recorded "gas chimneys" are commonly considered to be the result of hydraulic fracturing of an impermeable interval (Pyrak-Nolte, 1996; Heggland, 2005; Loseth et al., 2011; Hustoft et al., 2007, 2010; Cevatoglu et al., 2015). Hydraulic fractures develop when pore pressure exceeds the sum of the minimum lateral stress and the tensile strength of the sediment above and propagate upwards perpendicular to the direction of the minimum lateral stress (Phillips, 1972; Cosgrove, 1995; Hustoft et al., 2010; Loseth et al., 2009, 2011). Because the geological signification of chimneys has already been well discussed in many previous studies (cf. Loseth et al., 2001; Berndt et al., 2003; Hustoft et al., 2010; Plaza-Faverola et al., 2010; Ho et al., 2016), we are focusing on the timing of chimney formation and their nucleation in interaction with PFs.

5.2.1 Timing of chimney formation related to PFs

The timing of chimney formation is suggested to be recorded by their associated fluid flow features, which formed at chimney topmost terminations when hydrocarbon-charged fluid reached the palaeo seafloor: 1) pockmarks/depression, 2) methane-related carbonates.

Chimneys connected to pockmarks have been suggested to have formed during catastrophic blow-out events on the seafloor (Judd and Hovland, 2007; Hustoft et al., 2010). A proposed modern analogue was observed when a pockmark 40 m in diameter and 7 m deep formed above a chimney while overpressured water was expulsed after 5 ½ months, from a deeper reservoir (Loseth et al., 2011). During an experiment on CO2 injection in reservoirs, a 10 m long chimney terminating in a 4.5m wide and 60m deep pockmark on the seafloor developed within 48 hours at a onshore test-site in Scotland (Cevatoglu et al., 2015). These studies demonstrate that chimneys terminating into pockmark or depressions can form within days. Similarly, PHAAs at the top of chimneys, interpreted as seep carbonates (Hustoft et al., 2007; Petersen, 2010; Plaza-Faverola et al., 2011; Ho et al., 2012a) precipitate at the sea floor over time (Regnier et al. , 2011). At geological time scale, PHAAs can be considered as a time marker for gas migration through chimneys to reach the paleo-sea floor. Because PHAAs and the associated chimneys extended exactly from the linear gas accumulation below, and because the gas accumulations are compartmentalized by the anisotropic PF cells; it implies that the PF networks must have formed prior to the gas accumulations, and hence, modulate the planform development of chimneys and the subsequent fluid features.

Some might hypothesize that the chimneys emanating from the lower part of a polygonal fault plane formed by overpressured gas expulsion at the upper tip of proto-faults, which were still in their development stage. This assumption is, however, inconsistent with the fact that many chimneys are modern, and currently active (as indicated by PHAAs and pockmarks at their topmost terminations on the present day seafloor), while the fault planes have already fully developed (at the end of the

Pliocene) with their upper tip propagated above the nucleation point of the chimneys. The nucleation point of the chimneys must therefore correspond to a level from which the fluid could not migrate further along the fault plane, and hence, it forced the gas to open a new migration path i.e. chimney.

5.2.2 Level of chimney nucleation and location of gas accumulation

As the nucleation site of linear chimneys is directly linked to the site of gas accumulation, we first investigate the stratigraphic location of gas accumulation by tracing the gas migration pathway prior to the accumulations. This is done by analysing the chimney's downward termination. Type-3 chimneys (31%) initiated within the PF tier as indicated by negative amplitude columns at their downward termination (Fig. 6d). In contrast, the downward termination of the major population of chimneys (Type-1) cannot be determined with precision because of signal attenuation downward. However, they still appear to root in the lower part of the tier or its base, suggesting that overpressured gas-charged fluids occurred around the lower boundary of the tier. Most probably, the gas-charged fluids leaked through Type-1 chimneys and emptied the reservoirs leaving none or only weak seismic signals. In contrast, residual gas is still present in the reservoir of Type 3 chimneys. Therefore, Type-3 chimneys are interpreted as an earlier stage of Type-1, before their gas exhausted. Now we investigate how gas migrated specifically into the lower part of PF tier or below. Because PF root levels can be variable and the presence of bright spots occurs at different horizons (within or below the lower fault tier) (cf. profiles in Appendix 6), it is suggested that gas below the PF tier migrates via the long roots of PFs into different permeable layers within the tier. As the exact stratigraphic levels of gas sources and migration pathways to the base of chimneys could not be identified, based on the region in which chimneys are rooted, we propose the following scenarios when gas migrated upwards from deeper sources: (1) Gas was trapped in strata along sealed tectonic faults below the tier, (2) gas migrated laterally and reached certain carrier beds intersected by long PFs and accumulated at the base of the PF tier (Appendix 7, 8a), or (3) gas migrated along the lower portion of the PFs to reach a permeable layer inside the lower tier (Appendix 8b). These three processes either happened solely or in combination with each other as a series of steps. In conclusion, the rooting position of the majority of chimneys suggests that, before the chimneys nucleation, gas migrated and accumulated preferentially in the lower part or at the base of the PF tier.

5.2.3 Gas trapping in the lower part of the PF tier

As supported by the statistical analysis presented herein, > 54% of chimneys stem from the region around the lower PF footwall. We therefore, infer that > 54% of the time gas accumulated in the footwall at the base of chimneys. It is the same for the 19% of chimneys that stem from the lower hanging wall. Three hypotheses account for the mechanism of preferential gas accumulation in the lower PF footwalls, and one for hanging walls: 1) the present of an impermeable regional seal, 2) the differential strain in fault blocks and 3) the stratigraphic position of permeable layers in fault blocks, and finally 4) the increase of local permeability.

1) The seismic record documents that gas is present in the lower part of PF Tier-2 over a vast area, below the regional impermeable, Intra-Pliocene barrier(Ho, 2013). The Intra-Pliocene barrier corresponds to the topmost boundary of free gas accumulations, and does not parallel the seafloor (blue dotted line in Fig. 4d). As a result, this impermeable barrier does not

likely represent bottom simulating reflectors (BSR) and is, hence, interpreted as of purely depositional origin. The presence of an Intra-Pliocene barrier can explain why gas preferentially accumulated in the lower part of Tier-2, however, the preferential accumulation in the footwall side of the faulted compartment still needs to be investigated.

2) Shear strain resulting from extension and normal faulting affects the hydraulic properties of rocks adjacent to the fault surface (Barnett et al., 1987). Extensional faulting induces significant shear strain and dilatancy (Zhang et al., 2009) which consequently enhances the porosity and permeability of the wall rocks (Barnett et al., 1987). Numerical modeling demonstrates that the lowest shear stresses occur in the footwall block near the basal tip of a normal fault and that the greatest shear stresses occur in the upper part of hanging wall blocks (Fig. 9a Zhang et al., 2009; Welch et al., 2009). These results match the conceptual model of Barnett et al. (1987) which shows that the lower parts of footwalls and the upper part of hanging walls are in a state of relative compressional strain, compared to the top of the footwall and base of the hanging wall (Fig. 9b). As Tier-2 was buried only a few tens of meters when PFs formed, it was very likely not lithified and the lower part of the footwall blocks could have experienced dilatation (Barnett et al., 1987). Therefore, the highest permeabilities would be expected to occur in the footwall of a normal fault near the basal fault tip where gas accumulation is expected to occur. In fact, the majority of Linear Chimneys emanate from the lower parts of the footwall, where gas columns (NHA) are observed (Fig. 6d).

3) An alternative explanation for the preferential accumulation of gas in the footwall blocks of the faults is purely geometric: with normal faults, the footwall block is upthrown with respect to the hanging wall, and its series usually raise or tilt upward along the fault (Fig. 9c). As a result, upward migration of gas tends to fill the footwall side of the faults.

4) For the second major population of chimneys (19%) that stem from the middle of grabens (hanging wall), it is likely that the outbreak point of overpressured fluid is located in the lower part of the graben, where gas is likely to have accumulated before exceeding the lithostatic pressure. In the hanging wall, deposits are likely under a compressional regime (Barnett et al., 1987; Welch et al., 2009). Thus, gas will not preferentially migrate into such a location. However, a controlling factor is suggested being needed to guide the direction of gas migration: fracturing in graben bottom areas lead to permeability increase and facilitate for trapping gas (Ho et al., 2016, Appendix 8). This phenomenon happens when graben sediment moves downward along curved, steepening upward faults during extensional faulting (Cloos, 1868; Fossen and Rørnes, 1996; Bose and Mitra, 2010). In the upper parts of a graben, extensional phenomena dominate, while the lower parts of the graben are subjected to compression where a compressional fold forms a structural trap.

The above elements are suggested to induce the formation of PF fault-bound traps in the lower part of a PF tier.

5.2.4 Nucleation of Linear Chimneys

Based on seismic observations and the hypothesis of gas migration into the specific part of a PF interval, as established above, a conceptual model for the formation of Linear Chimneys is proposed in below. The majority of Linear Chimneys stem from the lower PF footwalls (Fig. 7b) suggesting gas-charged fluids could not migrate along the upper portion of PFs while impermeable. The permeability of small faults in fine-grained marine sediments varies upon the changes in stress and resultant strain around faults (cf. laboratory experience of Kaproth et al., 2016). Therefore, the impermeability along the upper part of PFs can be explained by the stress state around the fault. In literature, numerical models of Nunn (2013) shows that fluid pressure might

not be high enough to maintain low effective stress in the upper fault zones. Therefore, the upper part of the fault remains closed. Other modeling results show that it is possible for the lower part of PFs to appear permeable and critically stressed in the contemporary stress field while the upper parts are neither permeable nor critically stressed (Wiprut and Zoback, 2000; Zoback, 2007). In the anisotropic stress area (salt tectonic area), the fact that overpressured fluid-generated stress in host rocks leading to propagation of planar fractures in PF hanging walls indicates that fluid pressure was not high enough to open the upper fault plane, but only high enough to overcome the minimum horizontal stress plus the fracture strength of the fault blocks (Delaney et al. , 1986; Kattenhorn et al., 2000). Therefore, once the gas trapped in the lower part of the PF footwalls (Fig. 10a-b) became overpressured, hydraulic fractures propagate from the footwall to pierce the overlying strata and breach the impermeable barrier. As a result, the chimneys were initiated and originated along the lower part of polygonal fault planes. Apart from overpressured fluid (gas) creating new fractures, overpressured gas may also pass through, filling pre-existing sub-vertical cracks/fractures in the hanging wall bottoms along the main fault surface (fig. 2, Gaffney et al., 2007). Fluids may also open and extend pre-existing sub-vertical cracks/fractures in the hanging wall bottoms along the main fault surface (Gaffney et al., 2007). This happens only if the pressure required for fluid enters into the hanging wall fractures was less than the one for creating a new fracture (Gaffney et al., 2007). Pore pressures in the PF bound traps decrease after the fractures propagate or extend, and the residual gas in the traps may re-equilibrate with lithostatic pressure (Zoback, 2007). Consequently, some free gas can remain in the lower part of the PFs at the downward termination of Linear Chimneys (Fig. 6c).

For chimneys originating within the lower part of PF grabens, gas might be compartmentalized in the damaged graben by the impermeable portion of the PF, therefore, not flow into the adjacent horsts (Appendix 7). Consequently, hydraulic fractures initiated in the graben centre and propagated upward along the central axis (Fig. 10c).

5.2.5 Chimney's linear planform geometry and fault orientation

The linear planform of chimneys and their evident spatial relationship to anisotropic polygonal faults suggest that gas migration and hydraulic fracture propagation are controlled BY the alignments of anisotropic PFs. Anisotropic PFs follow the orientation of salt tectonic structures indicating that the PFs are controlled by the stress field generated by the salt structures (Carruthers, 2012); while the presence of faults alone can perturb the surrounding stress field and affect the adjacent fracture propagation (Rawnsley et al., 1992). Thus, stress fields play a determinant role in both formation of anisotropic PFs and the planform geometry of chimneys. In the stratigraphic interval where PFs are devoid, the parallelism between the deep tectonic faults and the kilometric-scale Linear Chimneys in Syncline-0 (Fig. 7a), clearly demonstrate that chimneys propagate toward the direction that resulted from the perturbation of horizontal anisotropic stresses induced by the tectonic faults (cf. Nakamura, 1977). In such location, the horizontal stresses are not equal as the intermediate horizontal principal stress exceeds the minimum one (Cosgrove, 1995). Thus, the gas pressure was likely not strong enough to overcome the intermediate horizontal stress so the hydraulic fractures opened in parallel with it, and against the direction of the minimum horizontal stress (Cosgrove, 1995). As a result, the final chimneys are linear in planform and follow the strike of adjacent faults. In the smaller scale of polygonal faulted blocks, Linear Chimneys and anisotropic PFs are often aligned, such as in Synclines-2 and 3 (Fig. 4a; 6a). However, in a particular location above the ridge of Syncline-2, Linear Chimneys are aligned with a pseudo isotropic (less anisotropic)

PF network enclosed in a zone between two (strong) anisotropic PF patterns, one is parallel to the edge of Syncline-2 and the other has a "ladder"-like pattern in the center of Syncline-2 (Figs 4a, 6a, b; Appendix 3a). In this specific location although PF pattern is similar to isotropic polygonal faulted areas but the stress magnitude remains greater because of the tectonic extension (Carruthers, 2012). Given that in such an enclosed (pseudo) isotropic PF area, chimneys are still linear, all aligned parallel to their rooted PF and do not show strong preferred orientation (Fig. 6a). We therefore conclude that at tier-fault scale, the in-situ anisotropic stress of the nearest PFs has major influence on the orientation of Linear Chimneys than the local tectonic fault stress field. The combination of both anisotropic stress fields of tectonic and polygonal faults is suggested to be the main cause of linear planform chimneys with preferential orientations, as Linear Chimneys do not occur in areas where isotropic PFs are solely present. Finally, the lateral propagation of the kilometric-scale Linear Chimneys rarely impeded by faults are oriented roughly parallel to them and the chimneys can reach much greater lengths. In contrast, chimneys within polygonally faulted areas are much shorter horizontally (> 300m) (Fig. 8). This is because the distance for which hydraulic fractures can propagate laterally along a specific trajectory is limited by faults. This example likely demonstrates that the planform and orientation of chimneys can be affected simply by the stress field of a tectonic fault. In conclusion, tectonic stress controls the orientation of anisotropic PFs, and the in-situ stress of the PFs control the orientation of Linear Chimneys.

5.2.6 Model of fluid migration and Linear Chimney formation

Linear Chimney formation can be summarized in 6 steps (Fig. 11).

1. During the Pliocene, anisotropic PFs formed under the influence of an anisotropic stress field induced by adjacent (salt-) tectonic structures, and developed during the Pliocene.

2. Gas-charged fluids migrated vertically from deeper intervals along tectonic faults, and laterally into the permeable beds below or at the base of a PF tier (Fig. 11a).

3. Gas-charged fluids migrated upward along the lower root of PFs, then flowed into the lower part of the tier, and filled the highest permeable layers in the horst or the fractured apex of grabens where the permeability was higher than in the undamaged sediment (Fig. 11a-b). The pressure of gas-charged fluid was not strong enough for allowing it intrude the upper part of PFs. Further upward migration of gas-charged fluids in strata was prevented by the Intra-Pliocene impermeable interval.

4. Overpressure of gas-charged fluids attained the threshold value for hydraulic fracture propagation but insufficient to reactivate the fault.

5. Hydraulic fractures (i.e. chimneys) grew from the lower part of the PF footwall or hanging wall (Fig. 11c), throughout the end of the Pliocene to the Quaternary. These fractures were affected by the stress field around the closest fault and developed into linear planforms and parallel to adjacent faults (along the direction of the intermediate horizontal principal stress).

6. The linear outlet of chimneys on the seafloor was eroded by gas venting, producing linear depression, in which methane-derived authigenic carbonates precipitated and expressed by PHAAs on seismic records (Fig. 11d).

Solid Earth Discuss., https://doi.org/10.5194/se-2018-34
Manuscript under review for journal Solid Earth
Discussion started: 17 May 2018

5.3 Implications for petroleum exploration

5.3.1 Reconstruction of hydrocarbon leakage history by using Linear Chimneys

The analysis of Linear Chimneys allows access to information about palaeo activities of buried hydrocarbon systems, especially how gas-charged fluid interacted with pre-existing geological structures while migrating upward to the subsurface. Based on the analysis of linear venting structures, we attempt to reconstruct the hydrocarbon leakage regime in the study area. The occurrence of linear venting structures and gas concentrations predominantly in synclines indicate that synclines are sites of active fluid flow (Fig. 4d, 6b). The reason why gas preferentially concentrates within syncline in the Pliocene PF interval in this study area may because of coarse-grained sediments trapped in the syncline depocenters during that period. It is known that syncline faults cut down to deep turbidite channel reservoirs (Monnier et al., 2014). Venting structures occurring around the extensional faults of synclines suggest that these faults served as initial leakage pathways for gas-charged fluids to migrate upwards. If the amount of gas exceeds the accommodation volume of the faults, gas will migrate horizontally into shallow carrier beds beneath the PF Tier-2 and then use the deep-rooted PFs as further leakage pathways into the PF tier (Fig. 12a). This explains why gas accumulations occur within PF Tier-2 above the center of Syncline-3, mimicking the geometry of the polygonal cells (= traps) (Fig. 4e). Within the anisotropic PF network in all syncline location (e.g. Fig. 4e, 6b), the preferential orientation of linear gas accumulation and hydraulic fractures (i.e. Linear Chimneys) suggests that the direction of gas flowing and escaping within the tier was likely guided by anisotropic stress fields. In contrast, where anisotropic PFs are absent no Linear Chimneys occur. Therefore, gas-charged fluids are likely not being affected by anisotropic stresses and may migrate in random directions, until they reach a permeable bed or mechanically weak zone to break through (Fig. 12b). To summerise, the direction of fluid leakage in areas of anisotropic PF can be predicted by analyzing fracture and fault directions (Ho, 2013; Ho et al., 2013).

5.3.2 Reconstruction of palaeo stress directions

While linear fluid conduits originate from perturbation of the stress field, they can be used as indicators of the palaeo stress field. Normal faults propagate parallel to the intermediate principal stress, while hydraulic fractures open in the plane of the maximum and intermediate principal stresses (Cosgrove, 1995). For example, in Syncline-1, the orientation of the first-order PFs implies that the direction of the intermediate compressive stress initially followed the curvature of the northern edge of Syncline-1 (Appendix 4). However, the Linear Chimneys rather formed parallel to the curvature of the eastern edge. Therefore, at the moment overpressured gas-charged fluids escaped via hydraulic fractures, the intermediate stress direction switched from a northern curvature to an eastern curvature. Thus, the horizontal stress field re-oriented during leakage of gas-charged fluids after PF formation. Next to the NE side of Syncline-1 an extensional fault set that is observed to parallel the Linear Chimneys (Appendix 4), was re-activated during Quaternary (red starts in Fig. 2a; Ho, 2013). Because these tectonic faults were active during the same time as the linear conduits formed (see Fig. 11b), it is plausible that the re-orientation of the stress fields in Sycline-1 resulted from the movement of these faults. In conclusion, comparing the direction of first-order PFs and the direction of Linear Chimneys is useful for diagnosing the evolutional history of stress fields in the past.

Solid Earth Discuss., https://doi.org/10.5194/se-2018-34
Manuscript under review for journal Solid Earth
Discussion started: 17 May 2018

We have shown that the formation and orientation of gas chimneys was modulated by the stress field of faults, and that the kilometre-scale Linear Chimneys are parallel to the tectonic faults in Syncline-0 (Fig. 8a); these chimneys with their lateral tips connect to each other and constitute a complex Linear Chimney network at 9 Ma. Their top is marked by a radial-depressional network formed due to further leakage. Methane-related authigenic carbonates that precipitated within the depressional network, formed another complex PHAA network and highlighting the radial geometry of underlying chimney network (Fig. 8b). Therefore, the subsequent flow structures associated with the chimneys that have the same planform also appear to be useful to determine the palaeo principal stress directions.

6 Conclusions

The anisotropic stress attributed to perturbations of the regional stress field by faults and salt diapirism, controls the orientation of PFs, which in turn impacts gas-charged fluid migration, leakage pathways and ultimately the geometry of gas leakage conduits and associated expulsion features at the seafloor. The mechanism of Linear Chimney formation is summarised as follows:

1) PF blocs form fault-bound gas traps in the lower part of PF tiers.

2) The location of these traps determines the site of gas leakage and hence, the nucleation site for vertical chimneys. 3) Linear Chimneys nucleating along the lower part of polygonal fault planes document that gas-charged fluids did not migrate along the upper portion of PF planes, which, therefore, appear to be impermeable.

4) Fluid expulsion features making the upper termination of chimneys at the palaeo sea floor (pockmarks, depressions and seep carbonates) date chimney formation from the End Pliocene to the Present. Polygonal faulting initiated in the shallow depth range from 50 to 100 ms TWT below the seafloor during Early Pliocene pre-date Linear Chimneys.

5) Orientation of chimneys is mainly determined by the orientation of the intermediate principal stress around the closest fault. Overpressured gas-charged fluids break through the host rock by pushing aside the host rock towards the direction of lowest principal stress, consequently Linear Chimneys developed aligned and parallel to the intermediate horizontal principal stress, and hence tectonic and/or polygonal fault strike.

6) Under the same spectrum of venting dynamics, the morphologies of chimneys and associated fluid expulsion features at the sea floor (depressions, pockmarks, seep carbonates bodies) are circular. In (strongly) isotropic stress fields they are linear in anisotropic stress fields surrounding tectonic faults, salt structures and in anisotropic PF networks.

7) In-situ stress fields of PFs alone are not sufficient to induce preferential orientated Linear Chimneys, but anisotropic tectonic stress fields must be involved.

8) Linear Chimneys can be used as a tool to reconstruct previous stress directions in the same way as using preferential orientated PFs.

Competing interests. No competing interest

Solid Earth Discuss., https://doi.org/10.5194/se-2018-34
Manuscript under review for journal Solid Earth
Discussion started: 17 May 2018

Acknowledgements. We thank Total S.A. for providing data, funding and its partners for publication permission, and the Ministry of Science and Technology of Taiwan for the grant MOST1052914I002069A1. Our work is based on and extended from Chapter 6 of S. Ho's PhD. The scientific work was fully carried out in Total-S.A.-France and completed under its direction. S Ho thanks Benoit Paternoster for his supervision on Geophysics since 2007. S. Ho thanks J.A. Cartwright for his great interest in this work, Mads Huuse for reviewing S. Ho's PhD, Cardiff University for the partial PhD funding. Thanks for the uncountable supports/advice from Timothy Byrne, David Hutchings, Quentin Vannelle, Ludvig Löwemark and Char-Shine Liu. A special thanks goes to Sebastian C. for the enormous supports.

References

Barnett, J. A., Mortimer, J., Rippon, J. H., Walsh, J. J., and Watterson, J.: Displacement geometry in the volume containing a single normal fault, AAPG Bulletin, 71, 925-937, 1987.

Berkson, J. M. and Clay, C.: Possible syneresis origin of valleys on the floor of Lake Superior, Nature, 245, 89-91, 1973.

Berndt, C., Bünz, S., and Mienert, J.: Polygonal fault systems on the mid-Norwegian margin: a long-term source for fluid flow, Geological Society, London, Special Publications, 216, 283-290, 2003.

Berndt, C., Jacobs, C., Evans, A., Gay, A., Elliott, G., Long, D., and Hitchen, K.: Kilometre-scale polygonal seabed depressions in the Hatton Basin, NE Atlantic Ocean: Constraints on the origin of polygonal faulting, Marine Geology, 332, 126-133, 2012.

Blouet, J.-P., Imbert, P., and Foubert, A.: Mechanisms of biogenic gas migration revealed by seep carbonate paragenesis, Panoche Hills, California, AAPG Bulletin, 101, 1309-1340, 2017.

Bose, S. and Mitra, S.: Analog modeling of divergent and convergent transfer zones in listric normal fault systems, AAPG Bulletin, 94, 1425-1452, 2010.

Bouriak, S., Vanneste, M., and Saoutkine, A.: Inferred gas hydrates and clay diapirs near the Storegga Slide on the southern edge of the Vøring Plateau, offshore Norway, Marine Geology, 163, 125-148, 2000.

Broucke, O., Temple, F., Rouby, D., Robin, C., Calassou, S., Nalpas, T., and Guillocheau, F.: The role of deformation processes on the geometry of mud-dominated turbiditic systems, Oligocene and Lower-Middle Miocene of the Lower Congo basin (West African Margin), Marine and Petroleum Geology, 21, 327-348, 2004.

Bureau, D.: Modalités mécaniques de la formation des intrusions de sable, Doctoral dissertion, Université du Maine, Le Maine, France, 2014.

Carruthers, D., Cartwright, J., Jackson, M. P., and Schutjens, P.: Origin and timing of layer-bound radial faulting around North Sea salt stocks: New insights into the evolving stress state around rising diapirs, Marine and Petroleum Geology, 48, 130-148, 2013.

Carruthers, T.: Interaction of polygonal fault systems with salt diapirs, doctoral dissertion, Cardiff University, Cardiff, UK, 489 pp., 2012.

Cartwright, J. A.: Episodic basin-wide hydrofracturing of overpressured Early Cenozoic mudrock sequences in the North Sea Basin, Marine and Petroleum Geology, 11, 587-607, 1994.

Cathles, L. M., Su, Z., and Chen, D.: The physics of gas chimney and pockmark formation, with implications for assessment of seafloor hazards and gas sequestration, Marine and Petroleum Geology, 27, 82-91, 2010.

Cevatoglu, M., Bull, J. M., Vardy, M. E., Gernon, T. M., Wright, I. C., and Long, D.: Gas migration pathways, controlling mechanisms and changes in sediment acoustic properties observed in a controlled sub-seabed CO 2 release experiment, International Journal of Greenhouse Gas Control, 38, 26-43, 2015.

Chopra, S. and Marfurt, K. J.: Seismic attributes for prospect identification and reservoir characterization, Society of Exploration Geophysicists and European Association of Geoscientists and Engineers, Tulsa, USA, 2007.

Clausen, J., Gabrielsen, R., Reksnes, P., and Nysaether, E.: Development of intraformational (Oligocene–Miocene) faults in the northern North Sea: influence of remote stresses and doming of Fennoscandia, Journal of Structural Geology, 21, 1457-1475, 1999.

Cloos, E.: Experimental analysis of Gulf Coast fracture patterns, AAPG Bulletin, 52, 420-444, 1968.

Coffeen, J.: Seismic exploration fundamentals, Penwell Press, Tulsa, USA, 1978.

Cosgrove, J.: The expression of hydraulic fracturing in rocks and sediments, Geological Society, London, Special Publications, 92, 187-196, 1995.

Davison, I., Alsop, I., Birch, P., Elders, C., Evans, N., Nicholson, H., Rorison, P., Wade, D., Woodward, J., and Young, M.: Geometry and late-stage structural evolution of Central Graben salt diapirs, North Sea, Marine and Petroleum Geology, 17, 499-522, 2000.

Delaney, P. T., Pollard, D. D., Ziony, J. I., and McKee, E. H.: Field relations between dikes and joints: emplacement processes and paleostress analysis, Journal of Geophysical Research: Solid Earth, 91, 4920-4938, 1986.

Duval, B., Cramez, C., and Jackson, M.: Raft tectonics in the Kwanza basin, Angola, Marine and Petroleum Geology, 9, 389-404, 1992.

Fossen, H. and Rørnes, A.: Properties of fault populations in the Gullfaks Field, northern North Sea, Journal of Structural Geology, 18, 179-190, 1996.

Fredrich, J. T., Coblentz, D., Fossum, A. F., and Thorne, B. J.: Stress perturbations adjacent to salt bodies in the deepwater Gulf of Mexico, in: Proceeding of SPE Annual Technical Conference and Exhibition, Denver, Colorado, 5 - 8 October 2003, SPE 84554, 2003.

Gaffney, E. S., Damjanac, B., and Valentine, G. A.: Localization of volcanic activity: 2. Effects of pre-existing structure, Earth and Planetary Science Letters, 263, 323-338, 2007.

Gay, A., Lopez, M., Berndt, C., and Séranne, M.: Geological controls on focused fluid flow associated with seafloor seeps in the Lower Congo Basin, Marine Geology, 244, 68-92, 2007.

Gay, A., Lopez, M., Cochonat, P., Séranne, M., Levaché, D., and Sermondadaz, G.: Isolated seafloor pockmarks linked to BSRs, fluid chimneys, polygonal faults and stacked Oligocene-Miocene turbiditic palaeochannels in the Lower Congo Basin, Marine Geology, 226, 25-40, 2006.

Gay, A., Lopez, M., Cochonat, P., Sultan, N., Cauquil, E., and Brigaud, F.: Sinuous pockmark belt as indicator of a shallow buried turbiditic channel on the lower slope of the Congo basin, West African margin, Geological Society, London, Special Publications, 216, 173-189, 2003.

Goulty, N.: Geomechanics of polygonal fault systems: a review, Petroleum Geoscience, 14, 389-397, 2008.

Heggland, R.: Detection of gas migration from a deep source by the use of exploration 3D seismic data, Marine Geology, 137, 41-47, 1997.

Heggland, R.: Definition of geohazards in exploration 3-D seismic data using attributes and neural-network analysis, AAPG Bulletin, 88, 857-868, 2004.

Heggland, R.: Using gas chimneys in seal integrity analysis: A discussion based on case histories. In: Evaluating Fault and Cap Rock Seals, P. Boult, J. K. (Ed.), AAPG Hedberg Series, 2, American Association of Petroleum Geologists, Tulsa, USA, 2005.

Henriet, J.-P., D'olier, B., Auffret, J., and Andersen, H.: Seismic tracking of geological hazards related to clay tectonics in the Southern Bight of the North Sea, IZWO Collected Reprints, 12, 1982.

Henriet, J., De Batist, M., and Verschuren, M.: Early fracturing of Palaeogene clays, southernmost North Sea: relevance to mechanisms of primary hydrocarbon migration, Generation, accumulation and production of Europe's hydrocarbons, 1, 217-227, 1991.

Henriet, J., De Batist, M., Van Vaerenbergh, W., and Verschuren, M.: Seismic facies and clay tectonic features of the Ypresian clay in the southern North Sea, Bulletin van de Belgische Vereniging voor Geologie, 97, 457-472, 1988.

Ho, S., Cartwright, J., and Imbert, P.: Vertical evolution of fluid venting structures in relation to gas flux, in the Neogene-Quaternary of the Lower Congo Basin, Offshore Angola, Marine Geology, 332, 40-55, 2012.

Ho, S., Cartwright, J., and Imbert, P.: The formation of advancing pockmarks arrays: an interplay between hydrocarbon leakage and slope sedimentation, in: Proceeding of American Association of Petroleum Geologists Annual Convention and Exhibition, Long Beach, USA, 18-20 September 2012, 1-10, 2012.

Ho, S.: Evolution of complex vertical successions of fluid venting systems during continental margin sedimentation, doctoral dissertion, Cardiff University Cardiff, UK, 2013.

Ho, S., Carruthers, T., Imbert, P., and Cartwright, J.: Spatial Variations in Geometries of Polygonal Faults Due to Stress Perturbations and Interplay with Fluid Venting Features, in: Proceeding of 75th EAGE Conference and Exhibition incorporating SPE EUROPEC 2013, London, UK, 10 - 13 June 2013, 1-6, 2013.

Ho, S., Carruthers, D., and Imbert, P.: Insights into the permeability of polygonal faults from their intersection geometries with Linear Chimneys: a case study from the Lower Congo Basin, Carnets Geol., 16, 17, 2016.

Hovland, M.: Elongated depressions associated with pockmarks in the western slope of the Norwegian Trench, Marine Geology, 51, 35-46, 1983.

Hovland, M.: Gas-induced erosion features in the North Sea, Earth Surface Processes and Landforms, 9, 209-228, 1984.

Hustoft, S., Mienert, J., Bünz, S., and Nouzé, H.: High-resolution 3D-seismic data indicate focussed fluid migration pathways above polygonal fault systems of the mid-Norwegian margin, Marine Geology, 245, 89-106, 2007.

Hustoft, S., Bünz, S., Mienert, J., and Chand, S.: Gas hydrate reservoir and active methane-venting province in sediments on< 20 Ma young oceanic crust in the Fram Strait, offshore NW-Svalbard, Earth and Planetary Science Letters, 284, 12-24, 2009.

Hustoft, S., Bünz, S., and Mienert, J.: Three-dimensional seismic analysis of the morphology and spatial distribution of chimneys beneath the Nyegga pockmark field, offshore mid-Norway, Basin Research, 22, 465-480, 2010.

Jacobs, C.: An appraisal of the surface geology and sedimentary processes within SEA7, the UK continental shelf, National Oceanography Centre, Southampton, Research and Consultancy Report No. 18, 127 pp., 2006.

Judd, A. and Hovland, M.: Seabed fluid flow: the impact on geology, biology and the marine environment, Cambridge University Press, Cambridge, UK, 2007.

Kaproth, B. M., Kacewicz, M., Muhuri, S., and Marone, C.: Permeability and frictional properties of halite-clay-quartz faults in marine-sediment: The role of compaction and shear, Marine and Petroleum Geology, 78, 222-235, 2016.

Kattenhorn, S. A., Aydin, A., and Pollard, D. D.: Joints at high angles to normal fault strike: an explanation using 3-D numerical models of fault-perturbed stress fields, Journal of Structural Geology, 22, 1-23, 2000.

King, R., Backé, G., Tingay, M., Hillis, R., and Mildren, S.: Stress deflections around salt diapirs in the Gulf of Mexico, Geological Society, London, Special Publications, 367, 141-153, 2012.

Laurent, D., Gay, A., Baudon, C., Berndt, C., Soliva, R., Planke, S., Mourgues, R., Lacaze, S., Pauget, F., and Mangue, M.: High-resolution architecture of a polygonal fault interval inferred from geomodel applied to 3D seismic data from the Gjallar Ridge, Vøring Basin, Offshore Norway, Marine Geology, 332, 134-151, 2012.

Ligtenberg, J.: Detection of fluid migration pathways in seismic data: implications for fault seal analysis, Basin Research, 17, 141-153, 2005.

Løseth, H., Wensaas, L., Arntsen, B., Hanken, N., Basire, C., and Graue, K.: 1000 m long gas blow-out pipes, in: Proceeding of 63rd EAGE Conference and Exhibition, Amsterdam, the Netherlands, 11 - 15 June 2001, P524, 2001.

Løseth, H., Gading, M., and Wensaas, L.: Hydrocarbon leakage interpreted on seismic data, Marine and Petroleum Geology, 26, 1304-1319, 2009.

Løseth, H., Wensaas, L., Arntsen, B., Hanken, N.-M., Basire, C., and Graue, K.: 1000 m long gas blow-out pipes, Marine and Petroleum Geology, 28, 1047-1060, 2011.

Mascle, J. and Phillips, J. D.: Magnetic Smooth Zones in the South Atlantic, Nature, 240, 80-84, 1972.

Monnier, D., Imbert, P., Gay, A., Mourgues, R., and Lopez, M.: Pliocene sand injectites from a submarine lobe fringe during hydrocarbon migration and salt diapirism: a seismic example from the Lower Congo Basin, Geofluids, 14, 1-19, 2014.

Moore, J. C., Orange, D., and Kulm, L. D.: Interrelationship of fluid venting and structural evolution: Alvin observations from the frontal accretionary prism, Oregon, Journal of Geophysical Research: Solid Earth, 95, 8795-8808, 1990.

Moss, J. L.: The spatial and temporal distribution of pipe and pockmark formation, Doctoral dissertion, Cardiff University, Cardiff, UK, 432 pp., 2010.

Nakamura, K.: Volcanoes as possible indicators of tectonic stress orientation—principle and proposal, Journal of Volcanology and Geothermal Research, 2, 1-16, 1977.

Nunn, J. A.: Pore-pressure-dependent fracture permeability in fault zones: implications for cross-formational fluid flow, Multidimensional basin modeling: AAPG, of AAPG Datapages, Discovery Series, 89-103, 2003.

Ostanin, I., Anka, Z., di Primio, R., and Bernal, A.: Identification of a large Upper Cretaceous polygonal fault network in the Hammerfest basin: Implications on the reactivation of regional faulting and gas leakage dynamics, SW Barents Sea, Marine Geology, 332, 109-125, 2012.

Petersen, C. J., Bünz, S., Hustoft, S., Mienert, J., and Klaeschen, D.: High-resolution P-Cable 3D seismic imaging of gas chimney structures in gas hydrated sediments of an Arctic sediment drift, Marine and Petroleum Geology, 27, 1981-1994, 2010.

Phillips, W. J.: Hydraulic fracturing and mineralization, Journal of the Geological Society, 128, 337-359, 1972.

Philippe, Y.: Angola SE Corner, Central Area And SW Corner : Teriary Regional Structural Synthesis, Elf Exploration, Internal report 72 pp., 2000.

Plaza-Faverola, A., Bünz, S., and Mienert, J.: Fluid distributions inferred from P-wave velocity and reflection seismic amplitude anomalies beneath the Nyegga pockmark field of the mid-Norwegian margin, Marine and Petroleum Geology, 27, 46-60, 2010.

Plaza-Faverola, A., Bünz, S., and Mienert, J.: Repeated fluid expulsion through sub-seabed chimneys offshore Norway in response to glacial cycles, Earth and Planetary Science Letters, 305, 297-308, 2011.

Plaza-Faverola, A., Bünz, S., and Mienert, J.: The free gas zone beneath gas hydrate bearing sediments and its link to fluid flow: 3-D seismic imaging offshore mid-Norway, Marine Geology, 291, 211-226, 2012.

Plaza-Faverola, A., Bünz, S., Johnson, J. E., Chand, S., Knies, J., Mienert, J., and Franek, P.: Role of tectonic stress in seepage evolution along the gas hydrate-charged Vestnesa Ridge, Fram Strait, Geophysical research letters, 42, 733-742, 2015.

Pollard, D. D. and Aydin, A.: Progress in understanding jointing over the past century, Geological Society of America Bulletin, 100, 1181-1204, 1988.

Pyrak-Nolte, L.: The seismic response of fractures and the interrelations among fracture properties, in: Proceeding of International journal of rock mechanics and mining sciences and geomechanics abstracts, 1996, 787-802.

Rawnsley, K., Rives, T., Petti, J.-P., Hencher, S., and Lumsden, A.: Joint development in perturbed stress fields near faults, Journal of Structural Geology, 14, 939-951, 1992.

Roberts, H. H. and Carney, R. S.: Evidence of episodic fluid, gas, and sediment venting on the northern Gulf of Mexico continental slope, Economic Geology, 92, 863-879, 1997.

Roberts, H. H., Hardage, B. A., Shedd, W. W., and Hunt Jr, J.: Seafloor reflectivity—an important seismic property for interpreting fluid/gas expulsion geology and the presence of gas hydrate, The Leading Edge, 25, 620-628, 2006.

Regnier, P., Dale, A. W., Arndt, S., LaRowe, D., Mogollón, J., and Van Cappellen, P.: Quantitative analysis of anaerobic oxidation of methane (AOM) in marine sediments: a modeling perspective, Earth-Science Reviews, 106, 105-130, 2011.

Sanz, P. and Dasari, G.: Controls on in-situ stresses around salt bodies, in: Proceeding of 44th US Rock Mechanics Symposium and 5th US-Canada Rock Mechanics Symposium, Salt Lake City, Utah, 27-30 June 2010, ARMA-10-169, 2010.

Sonnenberg, S., Underwood, D., Peterson, M., Finley, E., Kernan, N., and Harris, A.: Polygonal faults, Niobrara Formation, Denver Basin, in: Proceeding of AAPG Annual Convention and Exhibition, Calgary, Canada, June 19-22 2016, 51311, 2016.

Talukder, A. R.: Review of submarine cold seep plumbing systems: leakage to seepage and venting, Terra Nova, 24, 255-272, 2012.

Thrasher, J., Fleet, A. J., Hay, S. J., Hovland, M., and Düppenbecker, S.: Understanding geology as the key to using seepage in exploration: the spectrum of seepage styles. In: Hydrocarbon Migration and its Near-Surface Expression, AAPG Memoir 66, AAPG, Tulsa, USA, 1996.

Verschuren, M.: An integrated 3D approach to clay tectonic deformation and the development of a new 3D modeling method, University of Ghent, 359, 1992.

Welch, M. J., Knipe, R. J., Souque, C., and Davies, R. K.: A Quadshear kinematic model for folding and clay smear development in fault zones, Tectonophysics, 471, 186-202, 2009.

Wiprut, D. and Zoback, M. D.: Fault reactivation and fluid flow along a previously dormant normal fault in the northern North Sea, Geology, 28, 595-598, 2000.

Zhang, Y., Gartrell, A., Underschultz, J., and Dewhurst, D.: Numerical modelling of strain localisation and fluid flow during extensional fault reactivation: Implications for hydrocarbon preservation, Journal of Structural Geology, 31, 315-327, 2009.

Zoback, M. D.: Reservoir geomechanics: Earth stress and rock mechanics applied to exploration, production and wellbore stability, Cambridge Press, Cambridge, UK, 2007.

Solid Earth Discuss., https://doi.org/10.5194/se-2018-34
Manuscript under review for journal Solid Earth
Discussion started: 17 May 2018

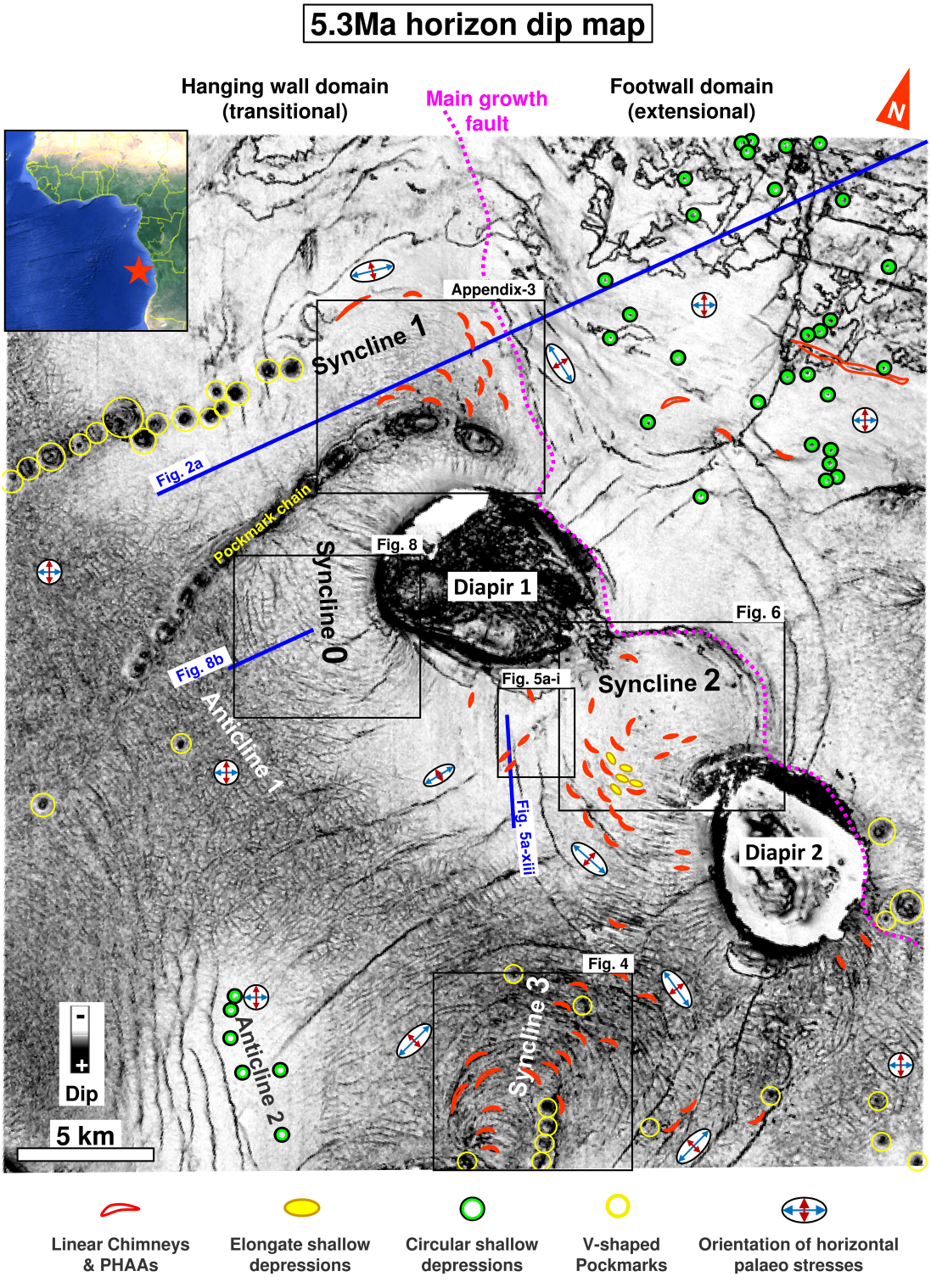

Figure 1. The study area and distribution of fluid expulsion structures shown on the dip map of horizon 5.3 Ma.

Solid Earth Discuss., https://doi.org/10.5194/se-2018-34
Manuscript under review for journal Solid Earth
Discussion started: 17 May 2018

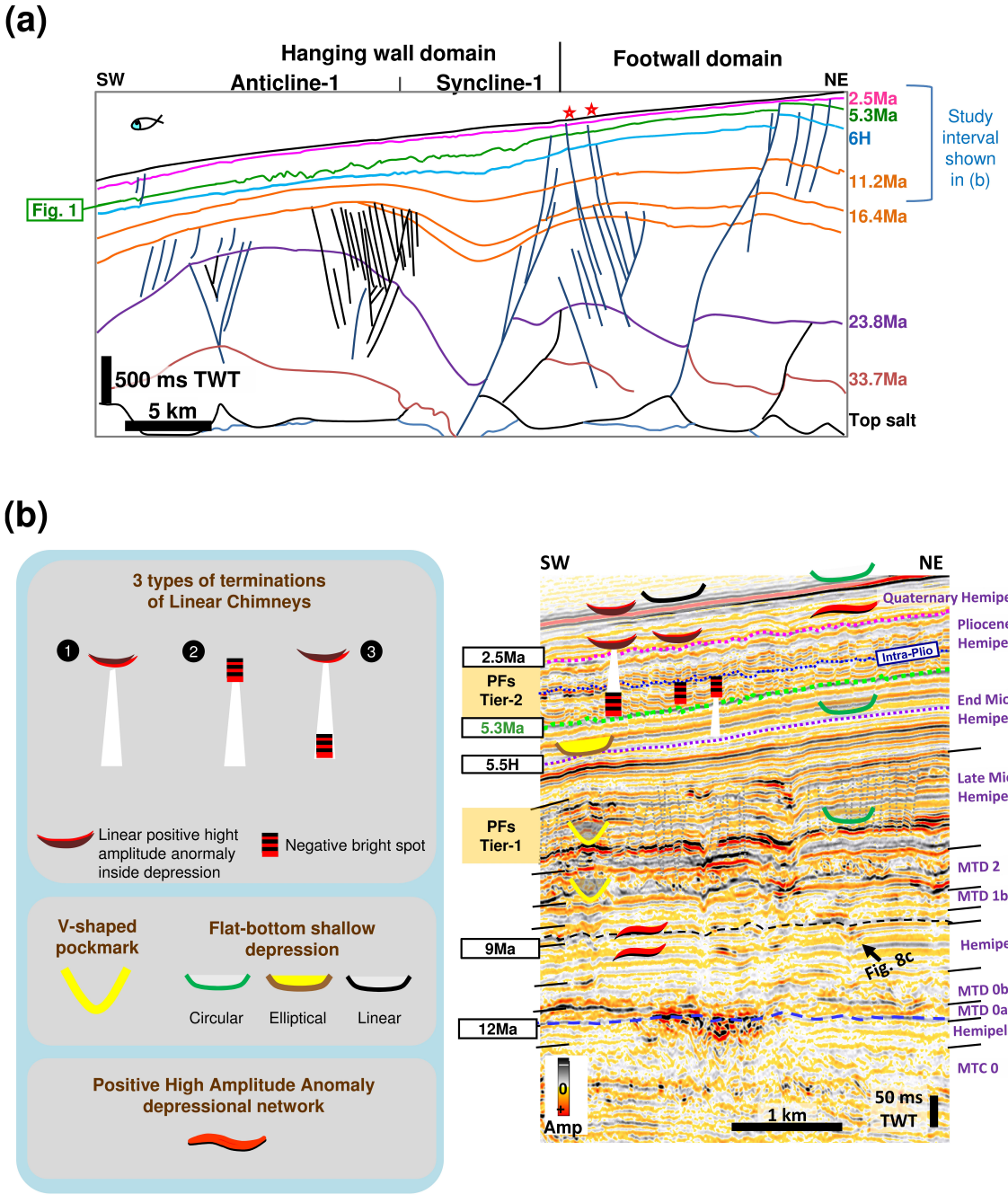

Figure 2. Geological setting of the study area. a) Line drawing of a regional profile. The red stars indicate the faults that reactivated during Quaternary. See figure 1 for location. b) Types of fluid expulsion structures (classification on the left) and their distribution along the detailed stratigraphy (seismic section on the right). "H" behind the digits stands for: "horizon" with an interpolated age. Adapted from Ho et al. (2012a) and Ho (2013).

Solid Earth Discuss., https://doi.org/10.5194/se-2018-34
Manuscript under review for journal Solid Earth
Discussion started: 17 May 2018

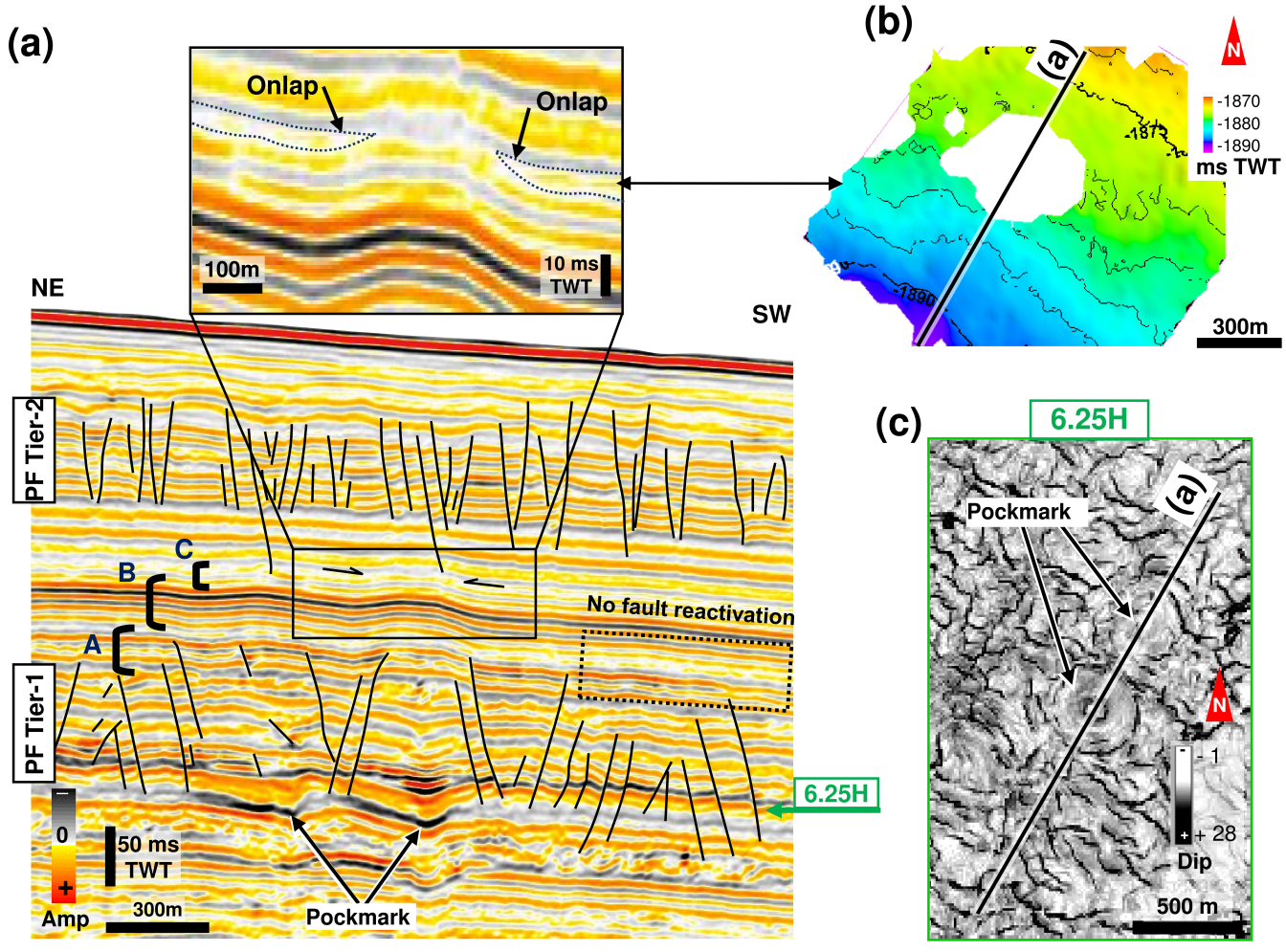

Figure 3. Direct evidence for the time when PFs ceased activity. a) Profile showing a circular PF developed in Tier-2 around a pockmark, and delimiting a horst right above the pockmark. A few faults propagate above the Tiers-2 (interval A); the first non-faulted strata (interval B) covers the relief of the horst with an isopach thickness; while the topmost reflection (in interval C) pinch-out on the positive topography, as indicated by black arrows. b) Two-way time map of the onlapping horizon (in interval C) showing a circular area absented of deposits above the horst location. c) A dip map of Tier-1 bottom showing circular PF that developed around a circular pockmark shown in (a) (Ho, 2013).

Solid Earth Discuss., https://doi.org/10.5194/se-2018-34
Manuscript under review for journal Solid Earth
Discussion started: 17 May 2018

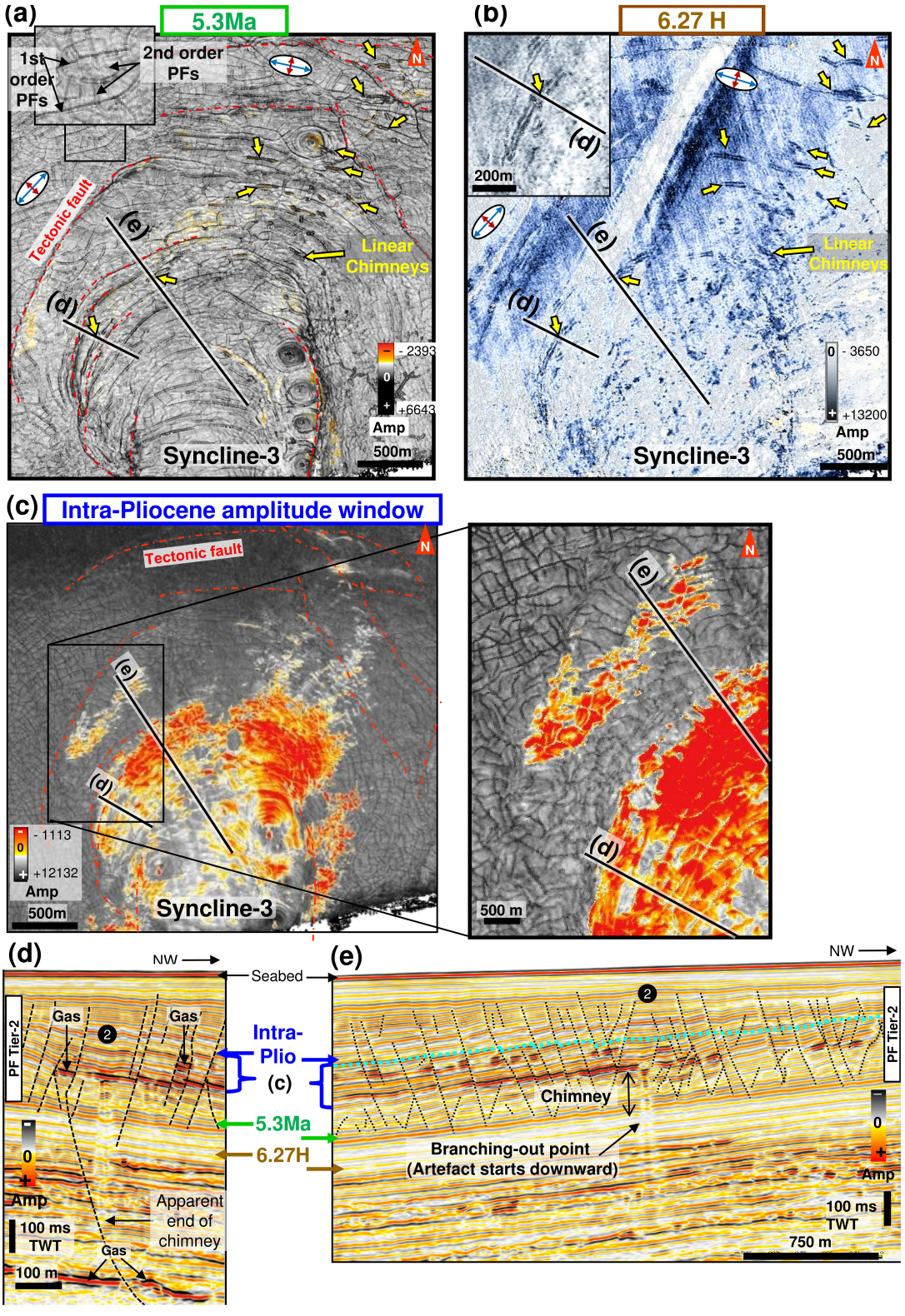

Solid Earth Discuss., https://doi.org/10.5194/se-2018-34
Manuscript under review for journal Solid Earth
Discussion started: 17 May 2018

Figure 4. Caption for previous page. Linear Chimneys above Syncline-3. a) Distribution of Linear Chimneys on a dip and amplitude attribute map of the basal surface of polygonal fault (PF) Tier-2 above Syncline-3. b) Amplitude map of horizon 6.27H c. 100 ms TWT below Tier-2 showing that Linear Chimneys are parallel to the strike of synclinal faults. c) Amplitude extraction of a window in the middle of Tier-2 showing km-scale accumulations of negative high-amplitudes within Syncline-3 and are bounded by extensional faults. Images sourced from Ho (2013; Ho et al., 2013). d) Linear Chimney emanating from a tectonic fault of the syncline. Black circle with digit indicate the type of chimneys. See red lines on maps b-c for location. e) Section view of distribution of gas accumulations within PF cells. Black circle with digit indicate the type of chimneys. See map (a-b) for location.

Solid Earth Discuss., https://doi.org/10.5194/se-2018-34
Manuscript under review for journal Solid Earth
Discussion started: 17 May 2018

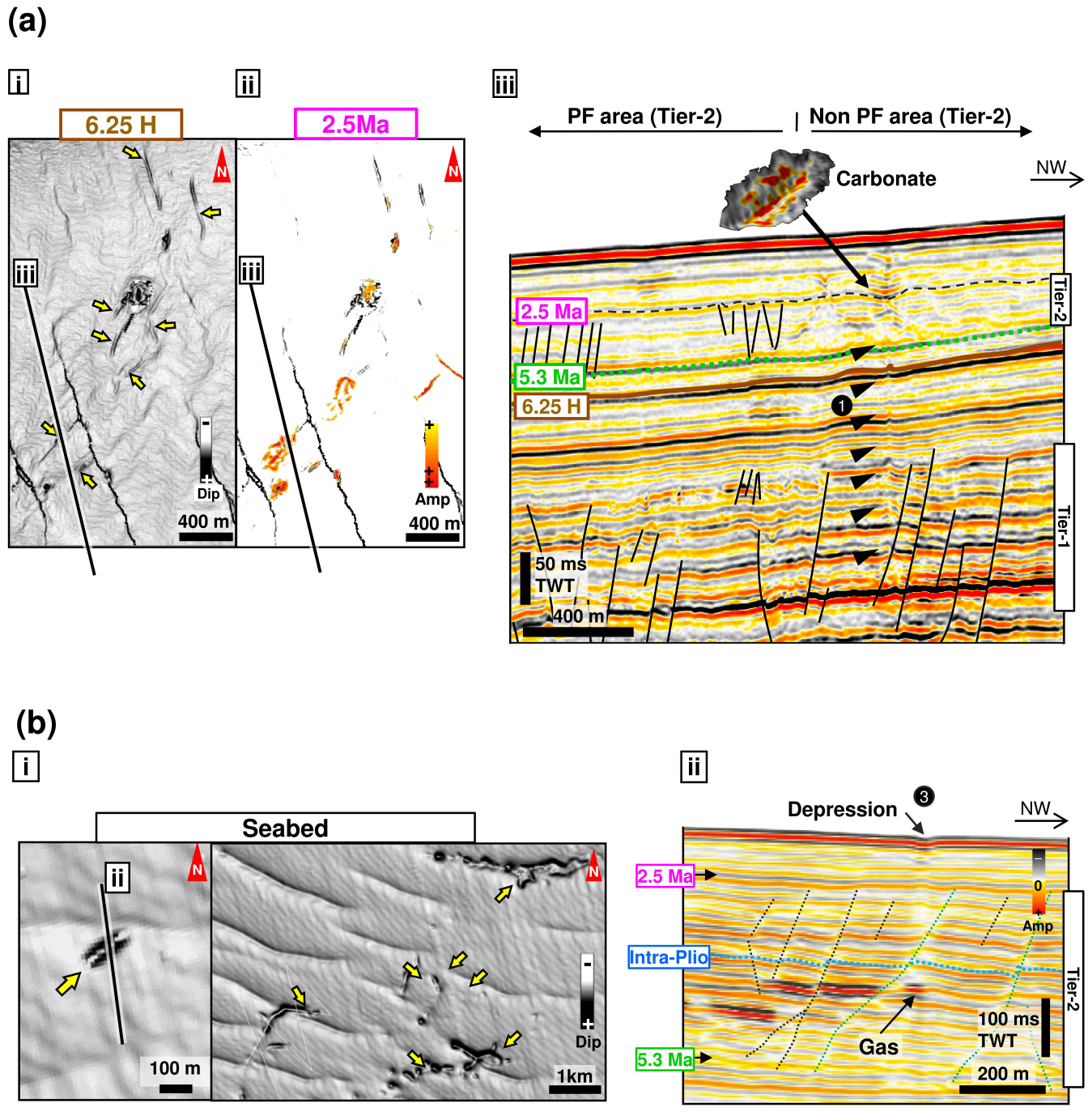

Figure 5. a) Group of Linear Chimneys with upward terminations in the upper Pliocene and emanating from Tier-1 of Middle Miocene. (i) Dip map of 6.25H showing the linear planform of chimneys (yellow arrows). (ii) Isolated positive high amplitude anomalies at the top boundary of initial Tier-2 (before the tier extension). They occur at the topmost termination of Linear Chimneys and are interpreted as methane-related carbonates. (iii) Seismic section showing the Linear Chimneys emanating from Tier-1. This section is a close-up of the

Solid Earth Discuss., https://doi.org/10.5194/se-2018-34
Manuscript under review for journal Solid Earth
Discussion started: 17 May 2018

thinning wedge studied in Ho et al. (2013). See location in (i) and full profile in appendix-6. b) Linear depressions at the present day seafloor. (i) The depressions at issue are indicated by yellow arrows and locally interfere with regularly spaced furrows of likely sedimentary origin. (ii) Seismic section shown on map (i) is across one depression, which occurs at the topmost termination of a Linear Chimneys emanating from Tier-1). Black circle with digit indicate the type of chimneys.

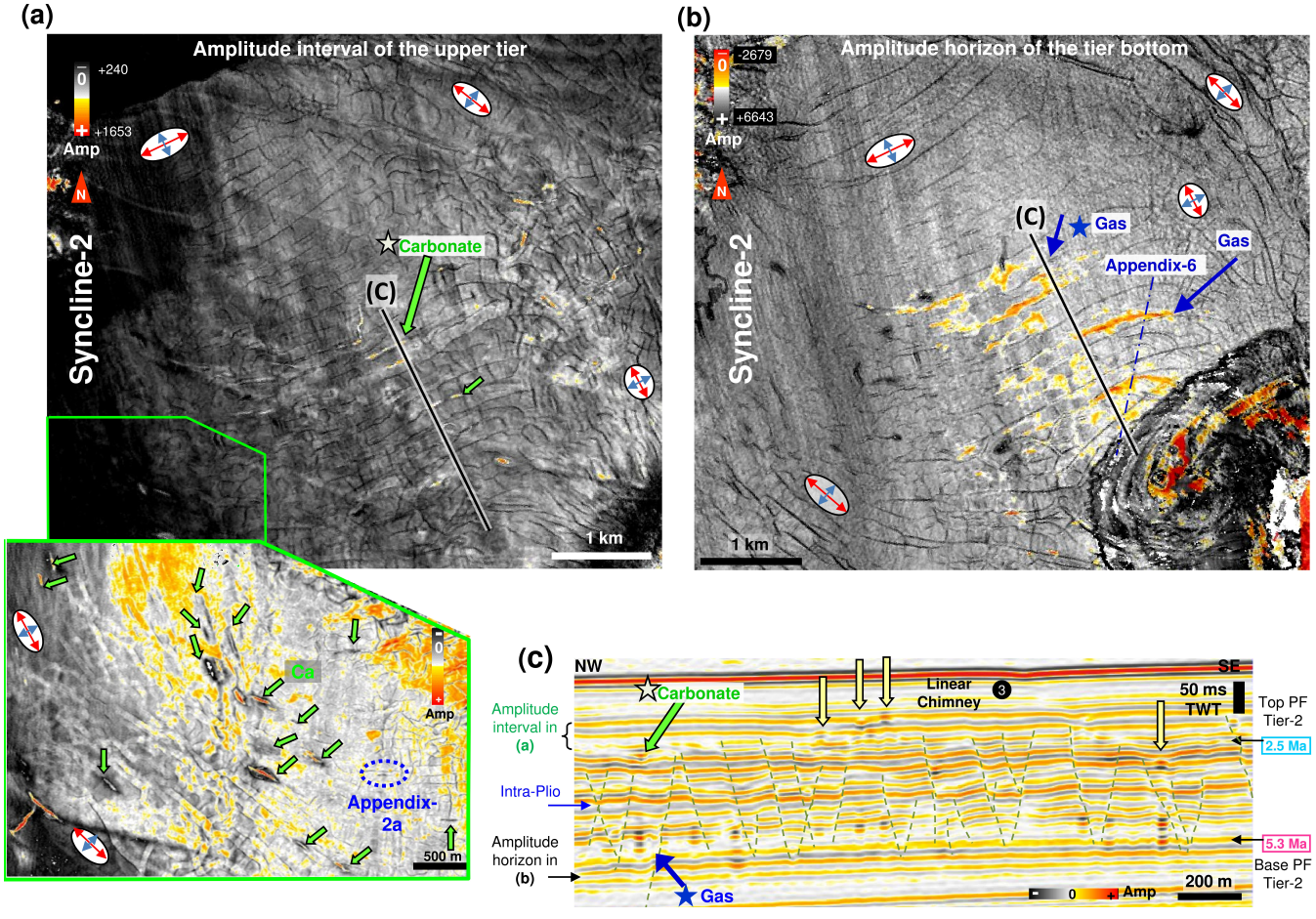

Figure 6. Alignment of Linear Chimneys parallel with polygonal faults in withdrawal Syncline-2. a) RMS amplitude extraction of a window in the upper portion of PF Tier-2 showing linear carbonates (red = highest amplitudes). See brackets in (c) for the vertical location. b) Amplitude map of the bottom horizon of PF Tier-2 bottom (red = high negative amplitude). c) Seismic section intersecting Linear Chimneys showing predominantly positive bright spots (Ca for Carbonate) at the top and negative bright spots at the bottom. Black circle with digit indicate the type of chimneys.

Solid Earth Discuss., https://doi.org/10.5194/se-2018-34
Manuscript under review for journal Solid Earth
Discussion started: 17 May 2018

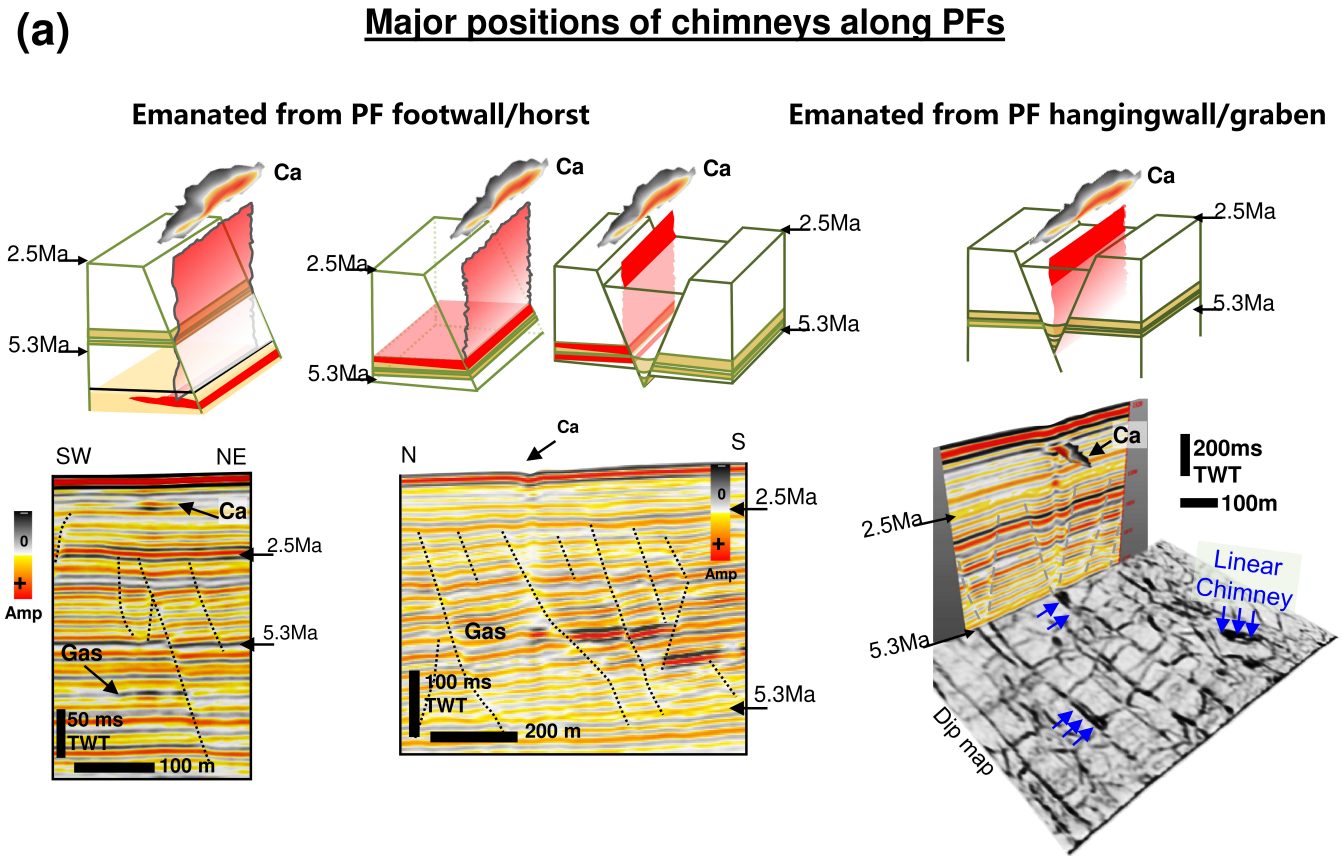

Figure 7. Caption next page.

[t]

Solid Earth Discuss., https://doi.org/10.5194/se-2018-34
Manuscript under review for journal Solid Earth
Discussion started: 17 May 2018

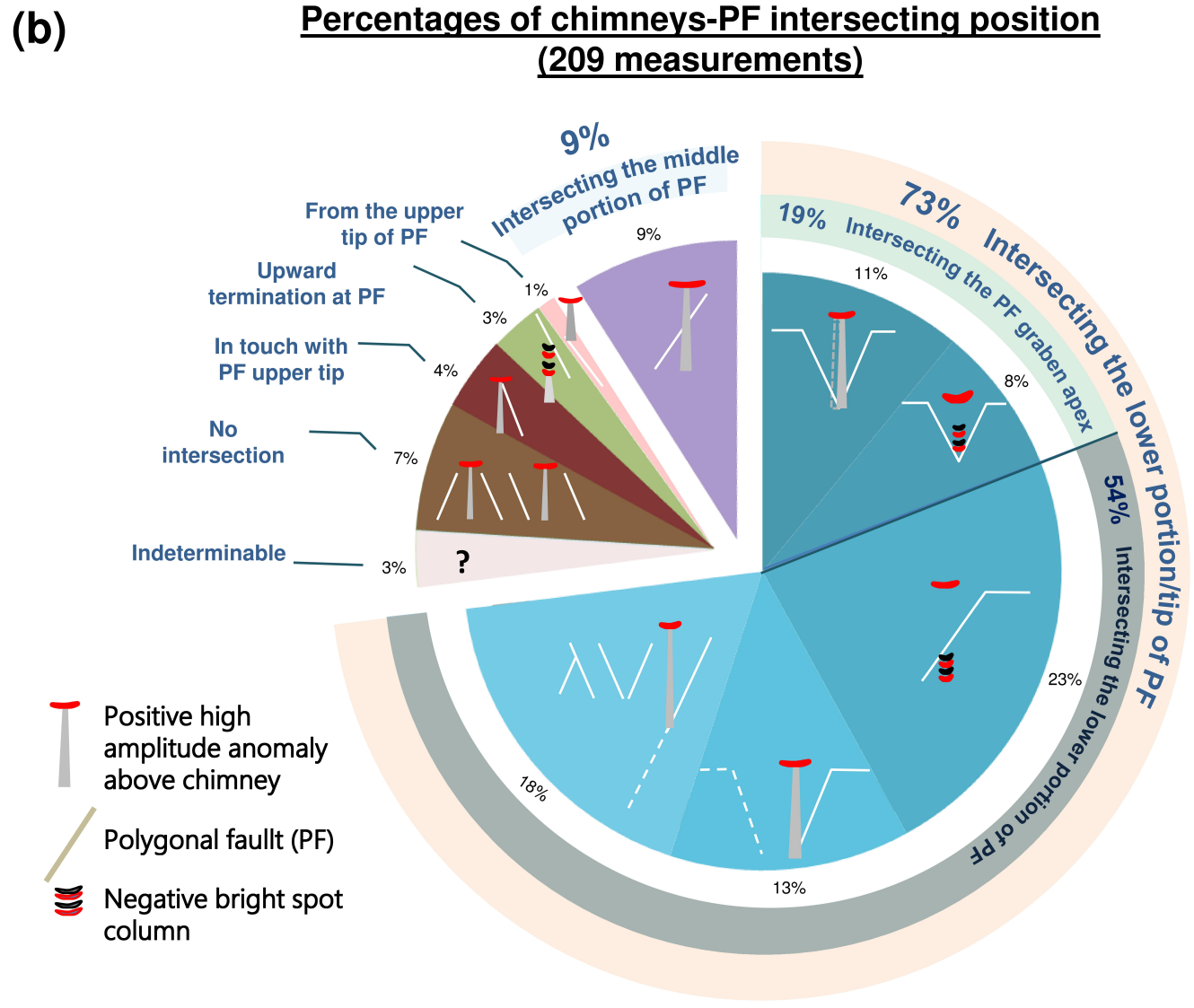

Figure 7. a) Group of Linear Chimneys with upward terminations in the upper Pliocene and emanating from Tier-1 of Middle Miocene. (i) Dip map of 6.25H showing the linear planform of chimneys (yellow arrows). (ii) Isolated positive high amplitude anomalies at the top boundary of initial Tier-2 (before the tier extension). They occur at the topmost termination of Linear Chimneys and are interpreted as methane-related carbonates. (iii) Seismic section showing the Linear Chimneys emanating from Tier-1. This section is a close-up of the thinning wedge studied in Ho et al. (2013). See location in (i) and full profile in appendix-6. b) Linear depressions at the present day seafloor. (i) The depressions at issue are indicated by yellow arrows and locally interfere with regularly spaced furrows of likely sedimentary origin. (ii) Seismic section shown on map (i) is across one depression, which occurs at the topmost termination of a Linear Chimneys emanating from Tier-1). Black circle with digit indicate the type of chimneys.

Solid Earth Discuss., https://doi.org/10.5194/se-2018-34
Manuscript under review for journal Solid Earth
Discussion started: 17 May 2018

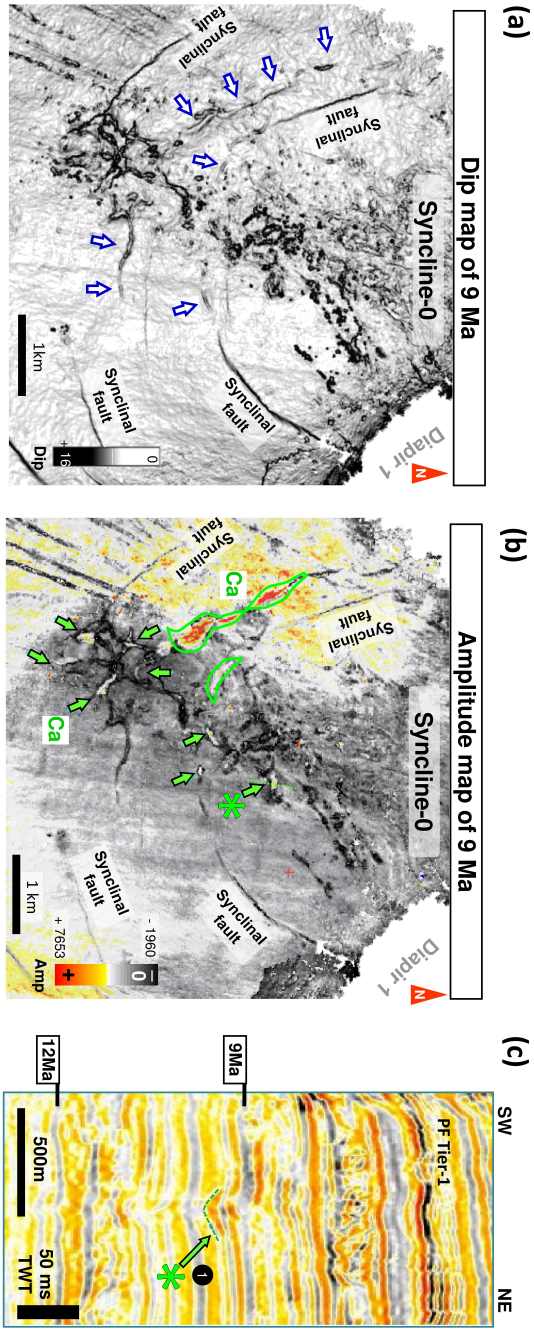

Figure 8. Kilometre-scale radial network of high positive amplitude depressions. a) Dip map and b) amplitude map of horizon 9 Ma showing the geometry of the network. Green star indicates a PHAA depression shown in (c). c) Close-up of the seismic section of figure 2b showing one PHAA within the network overlying a chimney. Black circle with digit indicate the type of chimneys. See green dotted line in (b) for location.

Solid Earth Discuss., https://doi.org/10.5194/se-2018-34
Manuscript under review for journal Solid Earth
Discussion started: 17 May 2018

Solid Earth
Discussions
Open Access
EGU

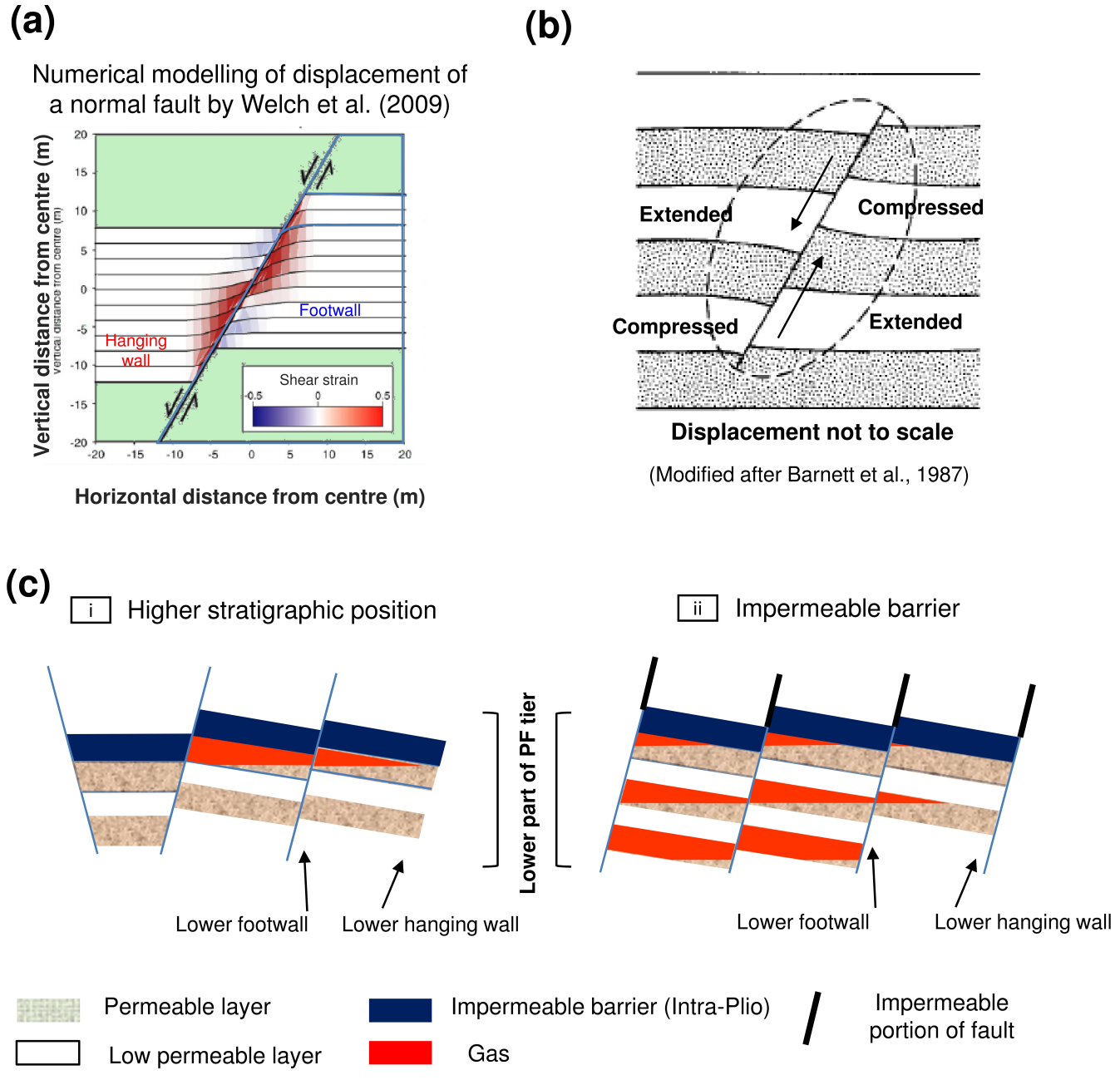

Figure 9. Causes of gas retention within the lower part of PF blocks. a) Diagram showing the magnitude of shear strain next to a normal fault (Modified after Welch et al, 2009). b) Displacement of horizontal beds by a normal fault and regions of relative extension and compression in the vicinity of a normal fault (Modified after Barnett et al., 1987). c) i: Higher stratigraphic position of permeable layers in PF footwalls (in compare to hanging wall) can cause preferential gas accumulation in such locations. ii: A thick enough impermeable barrier in the middle of the PF tier can prevent further upward migration of free gas.

Solid Earth Discuss., https://doi.org/10.5194/se-2018-34
Manuscript under review for journal Solid Earth
Discussion started: 17 May 2018

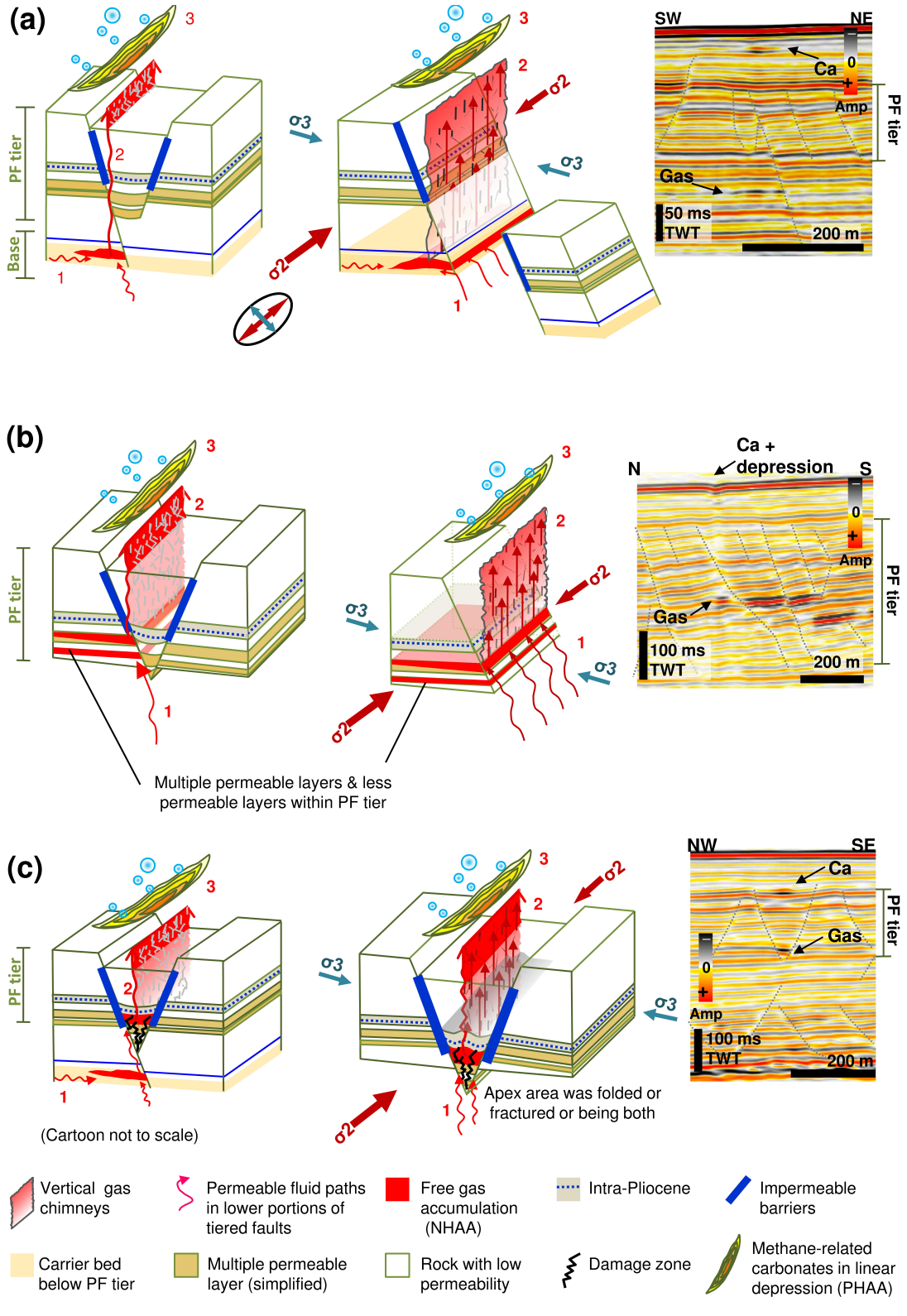

Solid Earth Discuss., https://doi.org/10.5194/se-2018-34
Manuscript under review for journal Solid Earth
Discussion started: 17 May 2018

Figure 10. Caption for previous page. Three different conceptual models of gas migration inside and below the PF tier (left column), based on seismic observations (examples are shown in the far right columns). Orientations of horizontal fault stress fields (local + in-situ) are indicated by arrows and stress ellipse. Free gas on seismic profiles is expressed by negative high amplitude anomaly (NHAA) while methane-related carbonates are expressed by positive high amplitude anomaly (PHAA). a) Below the PF tier where Linear Chimneys originate from; free gas is trapped by fault-bound traps formed by tectonic faults or deep-rooted PFs; b) Gas accumulation in the PF-bound traps in the lower part of PF footwalls; to notice the possible occurrence of multiple permeable layers filled by gas; c) Free gas trapped by lower hanging wall of PFs in which accommodation space was created by fractures or fold during subsidence.

Solid Earth Discuss., https://doi.org/10.5194/se-2018-34
Manuscript under review for journal Solid Earth
Discussion started: 17 May 2018

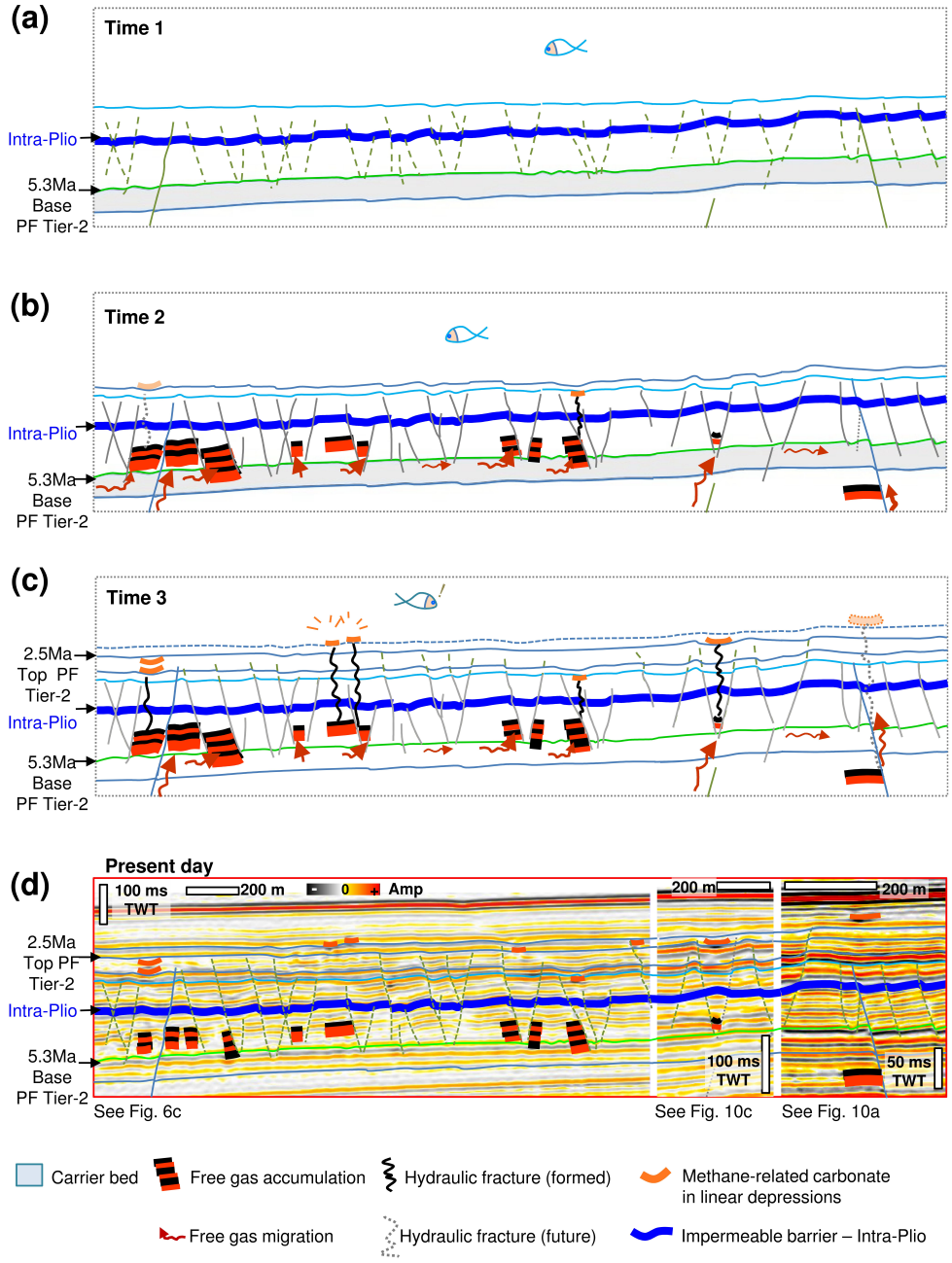

Figure 11. Conceptual model for the time steps of gas migration to the PF tier and formation of Linear Venting Systems. a) Initiation of PFs and deposition of impermeable barrier (Intra-Pliocene). b) PF tier and associated gas traps formed. Gas migrated along tectonic faults and reached the carrier bed below the PF tier first, then flowed into the PF-bound traps along the roots of PFs. c) Overpressure in these PF traps induced hydraulic fracture propagation up to the seafloor. Continuous gas expulsion induced the formation of depressions and methane-related carbonates above the fractures. PFs continue to propagate upwards during sedimentation. New generations of Linear Chimneys and depressions were formed.

Solid Earth Discuss., https://doi.org/10.5194/se-2018-34
Manuscript under review for journal Solid Earth
Discussion started: 17 May 2018

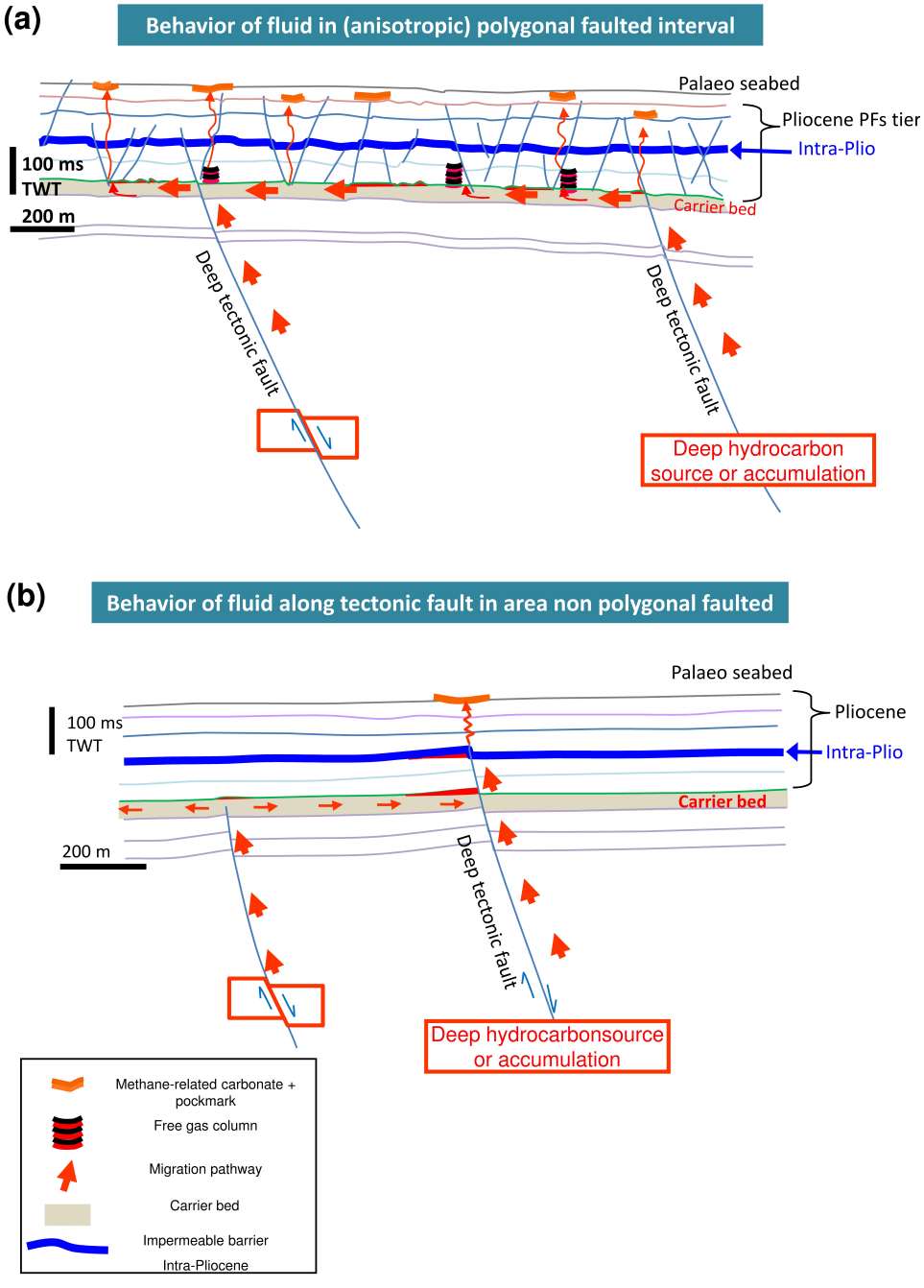

Figure 12. Drawings show the trajectories of gas migration branching out along the lower part of PF tier (a) but concentrating along a tectonic fault within the Pliocene interval (b).

Solid Earth Discuss., https://doi.org/10.5194/se-2018-34
Manuscript under review for journal Solid Earth
Discussion started: 17 May 2018

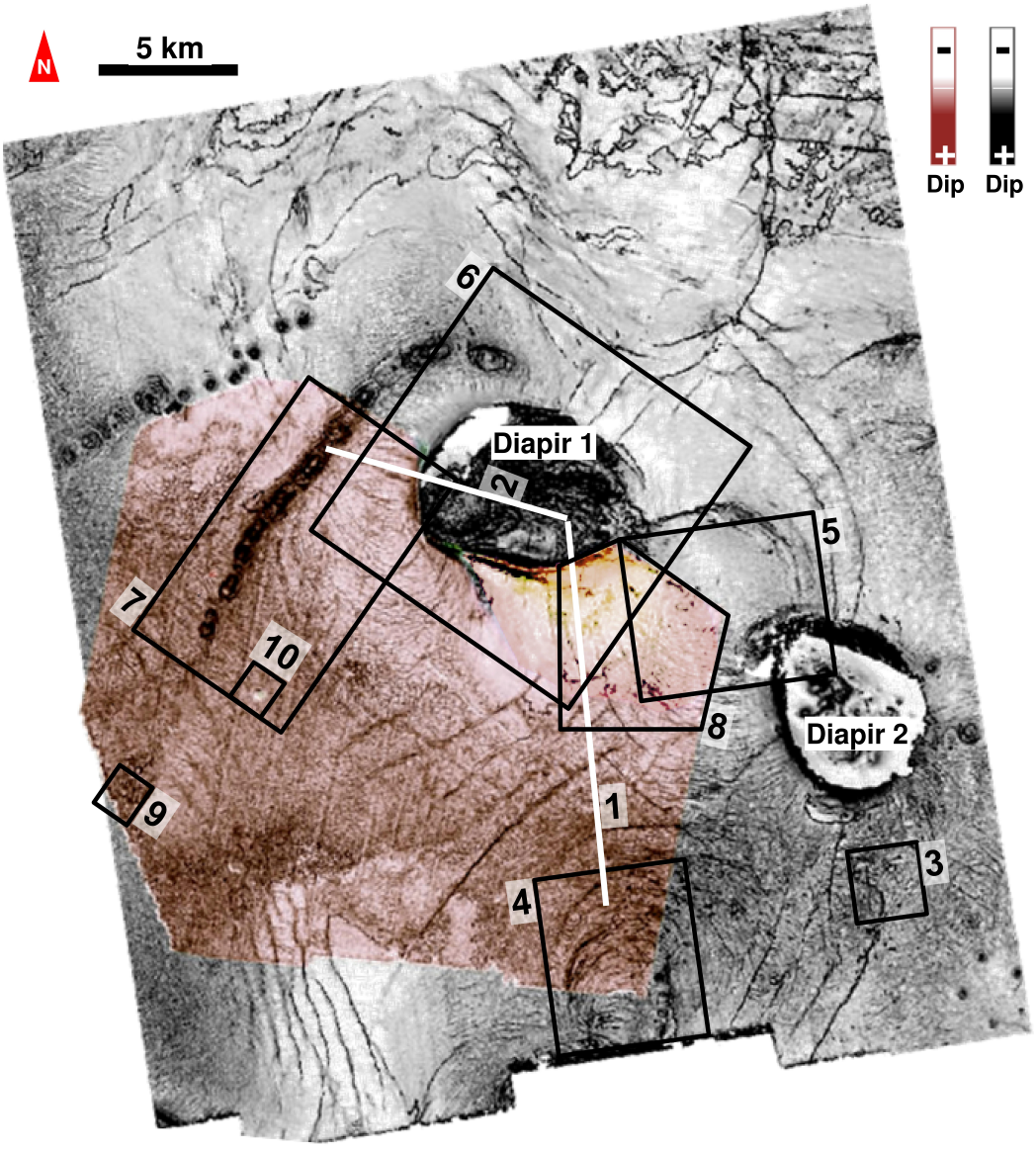

Figure A1. Appendix 1. The areas investigated in previous studies (Ho, 2013; Ho et al., 2012, 2013, 2016) are shown on the dip map of horizon 5.3Ma. Superposition of the high resolution survey (pink area) and the regional survey (grey area).

Solid Earth Discuss., https://doi.org/10.5194/se-2018-34
Manuscript under review for journal Solid Earth
Discussion started: 17 May 2018

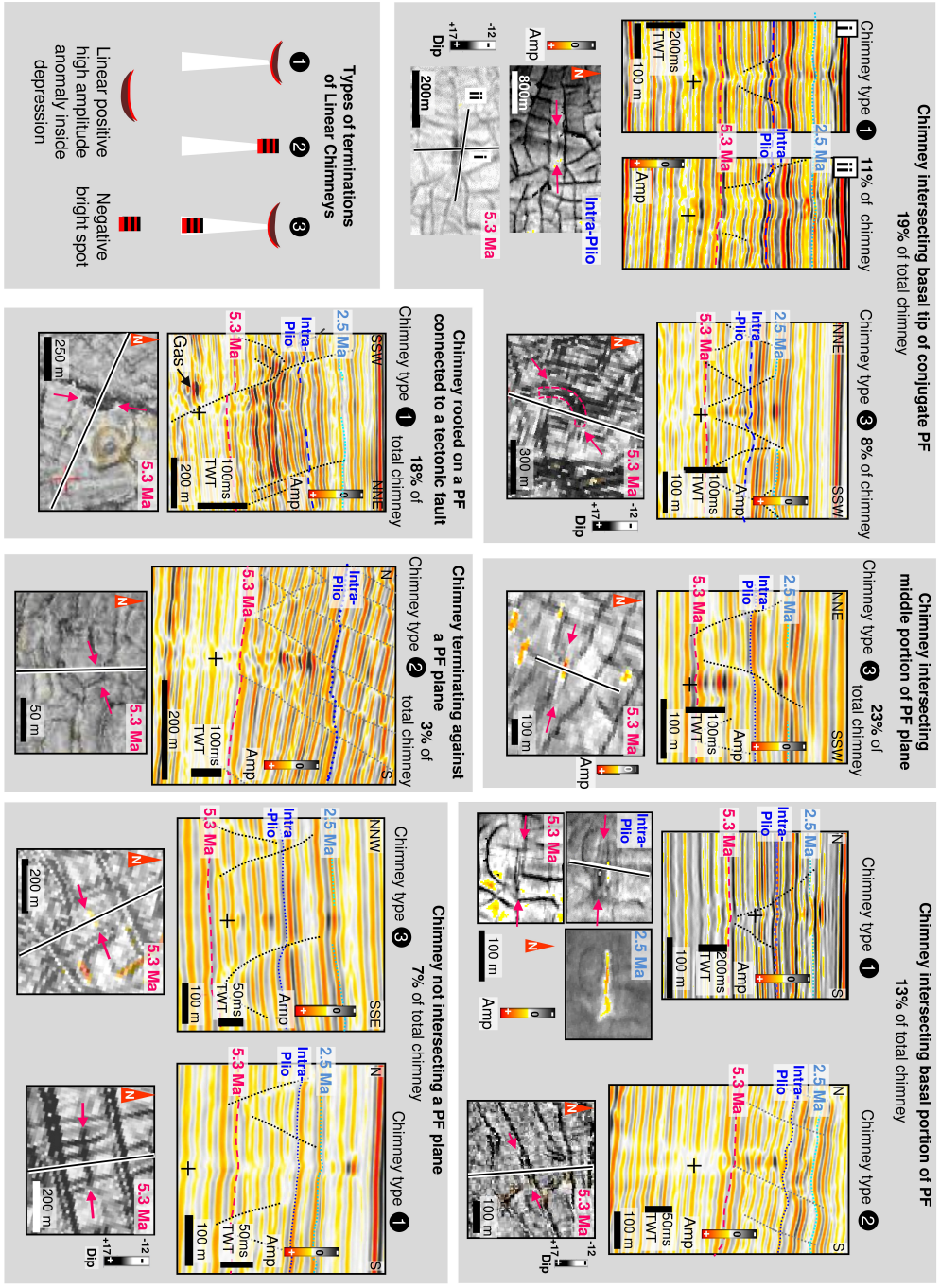

Figure A2. Appendix 2. Examples of chimneys intersecting and emanating from different parts of polygonal faults (PFs). The linear vents of Type-1, 2, 3 are labelled with black circles. The percentages correspond to the numbers of chimneys intersecting fault planes at specific positions (see pie chart in figure 5). The planform dimensions of the chimneys are shown on maps below each section. The apparent bases of chimneys are marked with crosses. See description in section 4.1.1.

Solid Earth Discuss., https://doi.org/10.5194/se-2018-34
Manuscript under review for journal Solid Earth
Discussion started: 17 May 2018

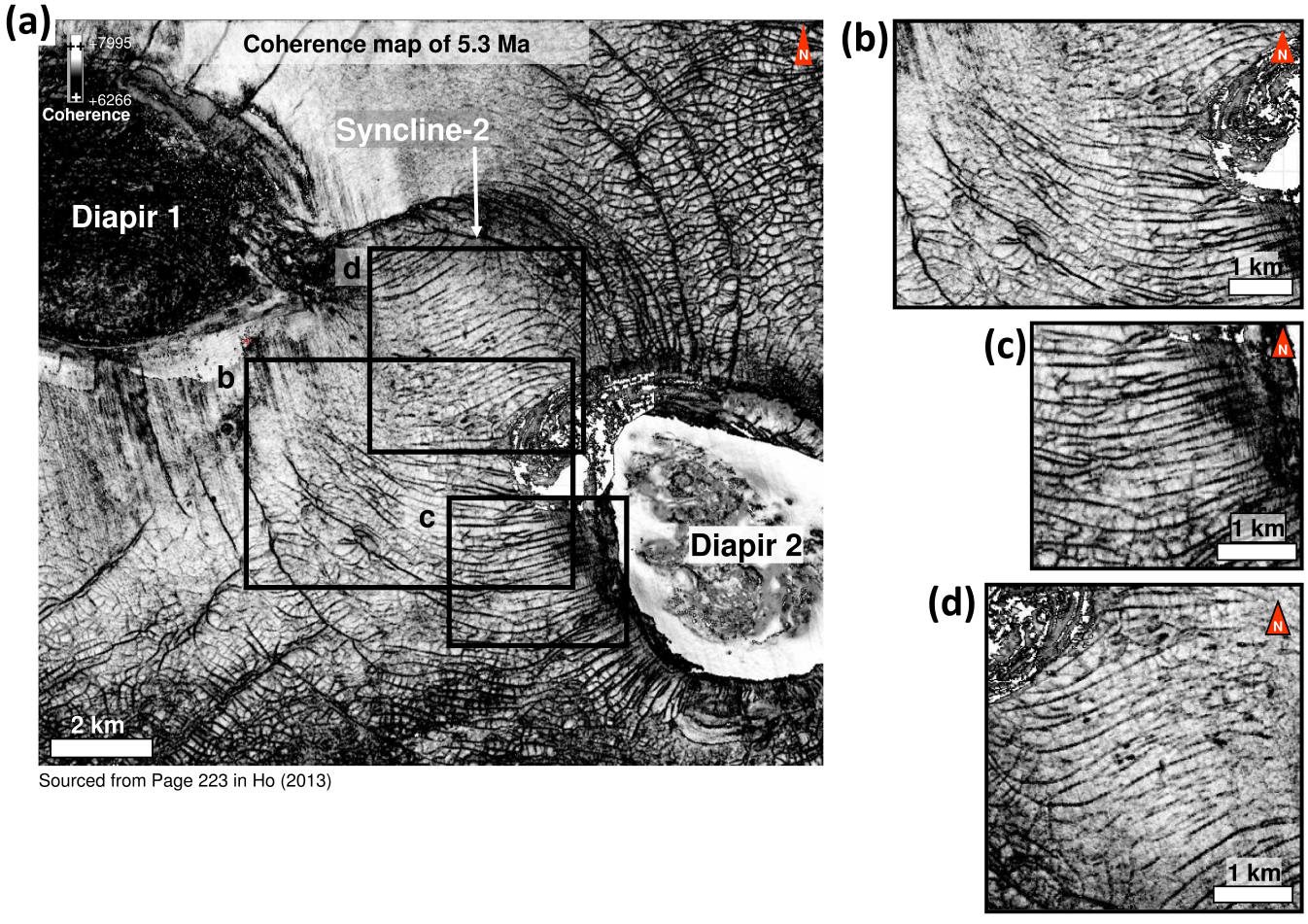

Sourced from Page 223 in Ho (2013)

Figure A3. Appendix 3. Anisotropic PF networks in which Linear Chimneys are found. a) Coherence attribute extracted onto the basal surface of PF Tier-2 showing the geometry and preferential alignment of PFs in withdrawal Syncline-2 and around Diapirs 1 and 2. b-d) Zooms of map in (a). Locations of maps are shown by coloured squares. Sourced from Page 223 in Ho (2013).

Solid Earth Discuss., https://doi.org/10.5194/se-2018-34
Manuscript under review for journal Solid Earth
Discussion started: 17 May 2018

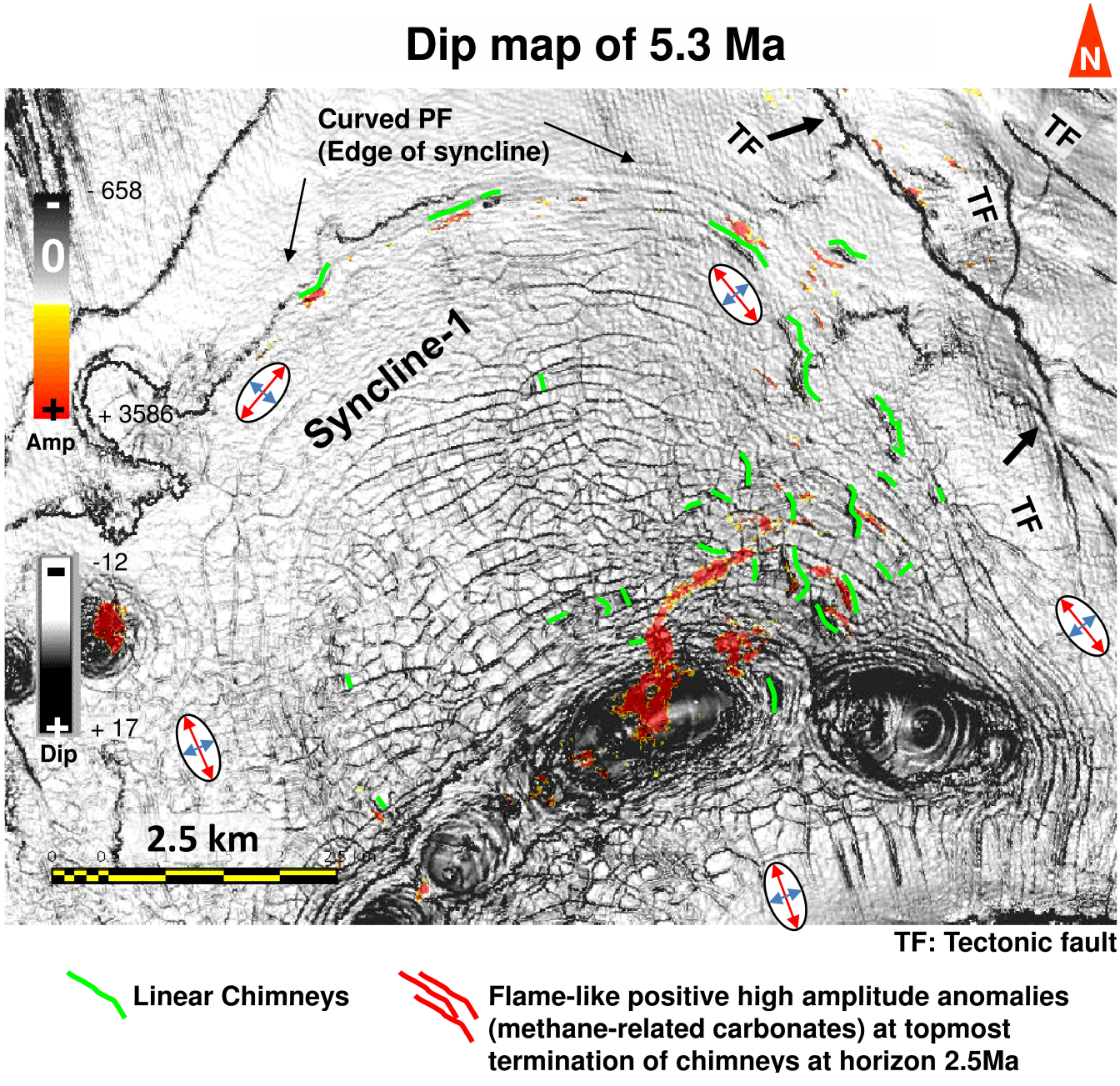

Figure A4. Appendix 4. Dip map of key horizon 5.3Ma in Syncline-1 location. Isolated positive high amplitude anomalies (PHAAs) interpreted as methane-related carbonates, at horizon 2.5Ma at the topmost terminations of Linear Chimneys, superimposed with the 5.3Ma dip map, i.e. the base of PFs Tier-2. Green lines highlight the locations of Linear Chimneys underlying the carbonate. Red amplitudes are "flame-like" PHAAs.

Solid Earth Discuss., https://doi.org/10.5194/se-2018-34
Manuscript under review for journal Solid Earth
Discussion started: 17 May 2018

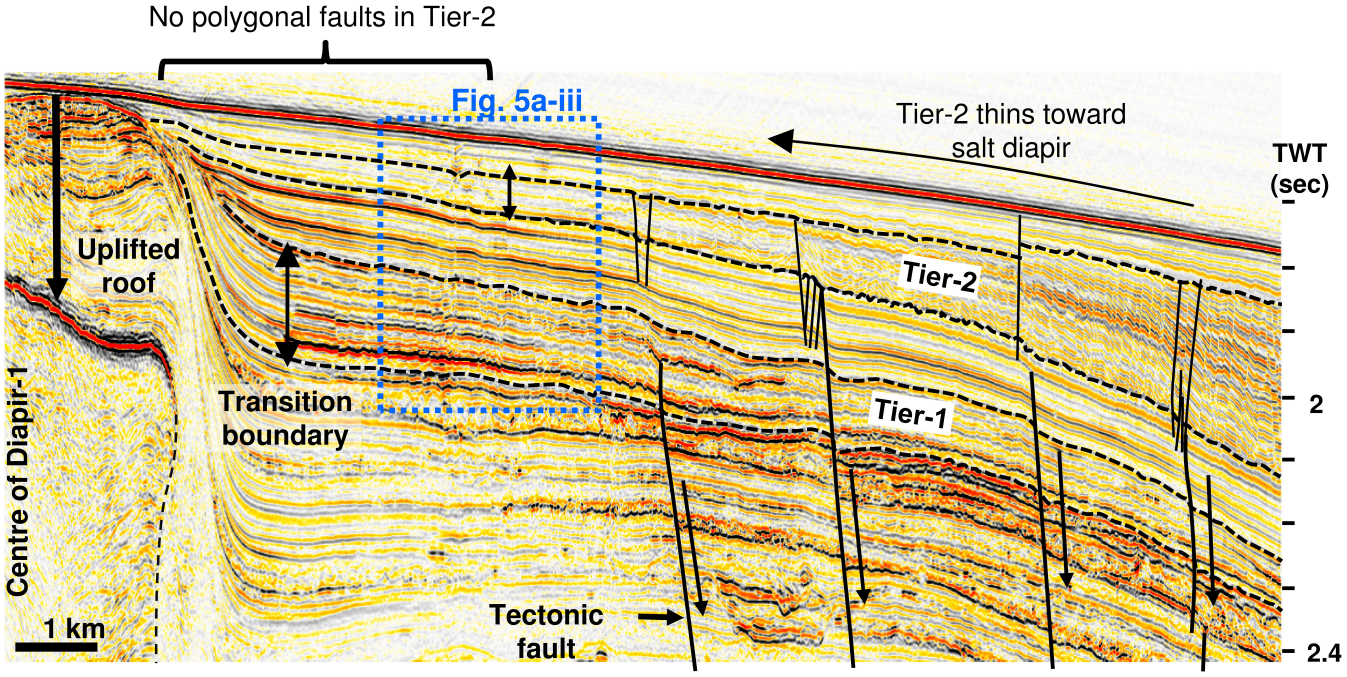

Figure A5. Appendix 5. Arbitrary seismic line intersecting the SE flank of Diapir-1 and showing the variable thickness of PF tiers. Syn-sedimentary growth wedges of Tier-1 and -2 are highlighted by black dot lines. Line location is labelled (1) in Appendix-A. The polygonal faults disappear progressively towards the pinch-out of the PF tiers beyond the black arrows, at the transitional boundary where the wedge thickness starts to be less than 60 ms . Note that PFs are absent in the pinch-out of Tier-2, but are present at the same location in Tier-1 below, where this tier reaches its maximum thickness (Ho et al., 2013). This may provide additional support for the theory of minimum thickness determining PF growth (Carruthers, 2012). This observation can serve as a reference example on PF growth. Image adapted from Ho et al. (2013).

Solid Earth Discuss., https://doi.org/10.5194/se-2018-34
Manuscript under review for journal Solid Earth
Discussion started: 17 May 2018

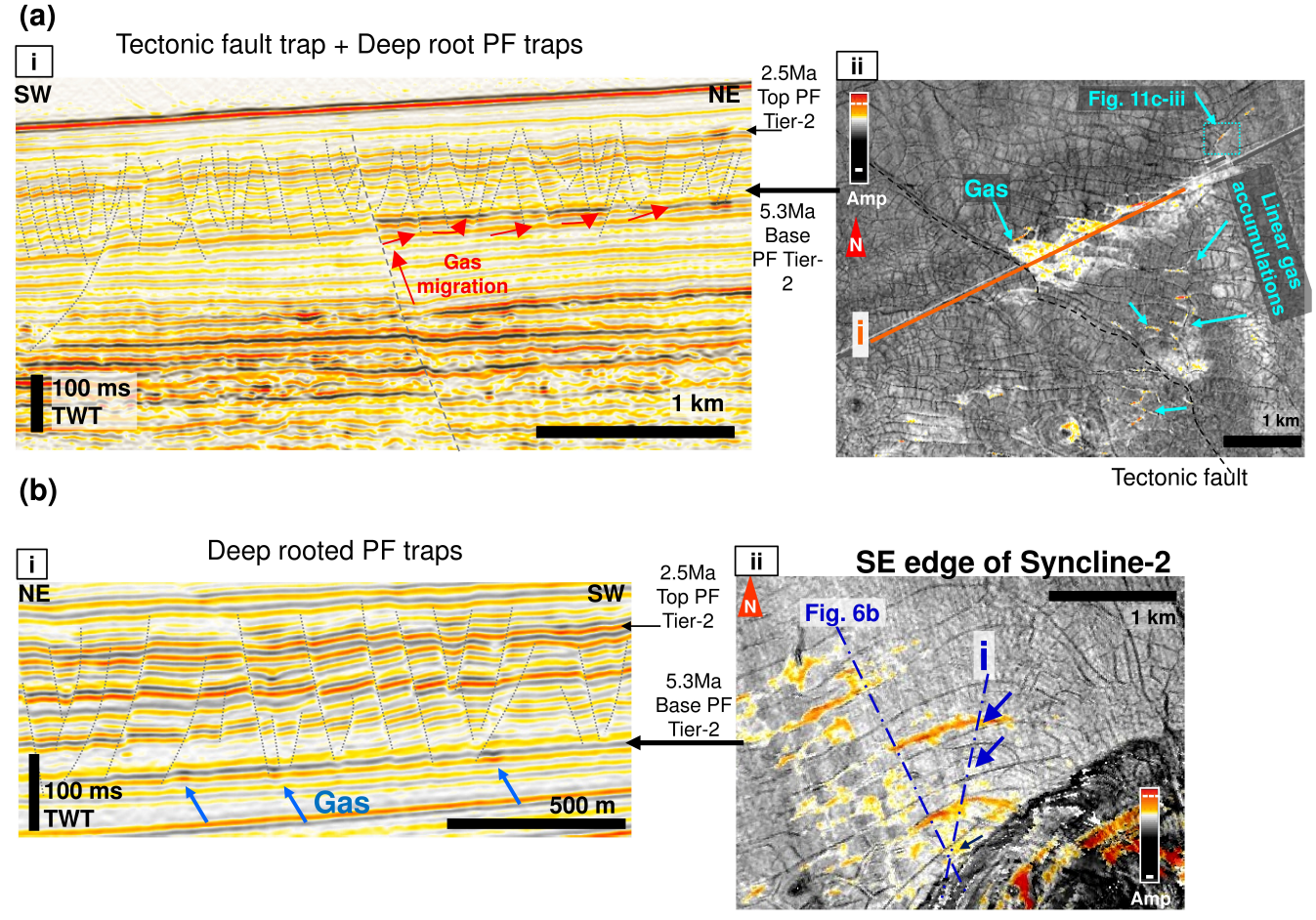

Figure A6. Appendix 6. Linear patches of negative high amplitudes interpreted to correspond to gas accumulation at the base of PF Tier-2. a) Free gas interpreted to have migrated along a tectonic fault and flowed preferentially into a permeable interval at the base of Tier-2 in the higher elevation as shown on (i). Note that the deep-rooted PFs extend deeper than the tier. (ii) The amplitude map along the base of Tier-2 shows that gas had actually filled the whole PF cells. b) Gas occurs around the bottom of deep-rooted long PFs as shown on (i), and exhibit linear planforms on the amplitude map of Tier-2's base (ii).

Solid Earth Discuss., https://doi.org/10.5194/se-2018-34
Manuscript under review for journal Solid Earth
Discussion started: 17 May 2018

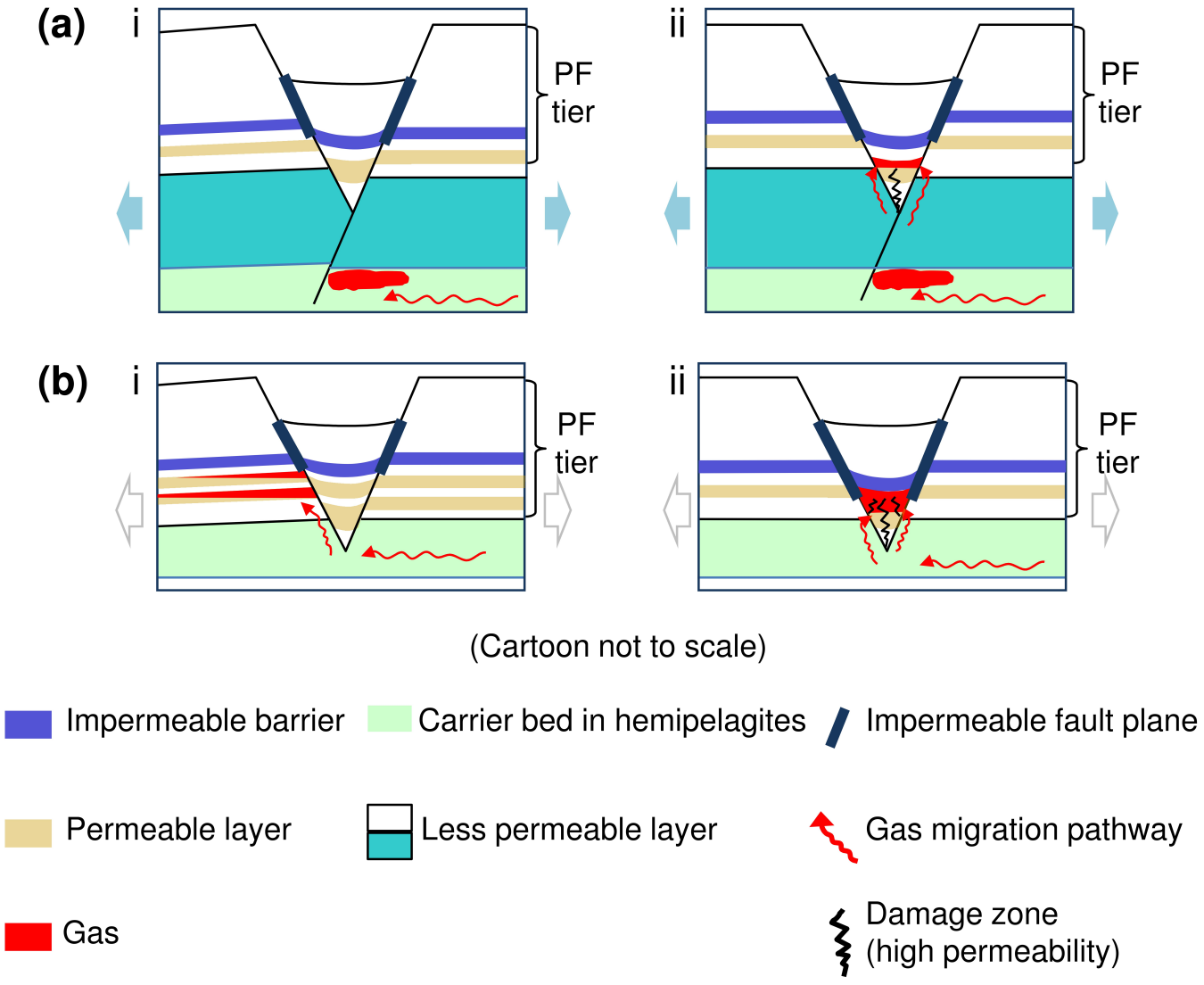

Figure A7. Appendix 7. Gas migration into the PF tier. a) Conceptual model for free gas migration into the permeable layer in the lower part of polygonal fault Tier-2 from an underlying carrier bed. Bold black lines denote the segments of PFs interpreted as impermeable. Cartoon not to scale. a) Case where the carrier bed occurs beneath the basal tier surface of the PF tier (the carrier bed thickness can extend beyond the bottom of the cartoon). First-order PFs (i.e. those that have propagated under the influence of tectonic stresses) have propagated beneath the regional tier surface and have intersected the carrier bed. (i) Gas migrated into the permeable layer of the footwall and (ii) into the hanging wall. Gas migrated into the hanging wall apex is likely because of the increase of permeability induced by apex damaging. b) Cases where the carrier bed occurs at the base of a polygonal fault tier. (i) Gas migrated into the permeable layer in the footwall via a permeable polygonal fault plane. (ii) Gas migrates into the overlying permeable layer in the fractured hanging wall when it is juxtaposed against the carrier bed.